

Internal Kinematics of Galaxies

ASTR 511

Overview

- Overview
- Observational methods and constraints
- Kinematics of Early Type Galaxies
- Kinematics of Late Type Galaxies
- The Milky Way
- Dwarf Spheroidals

Kinematics

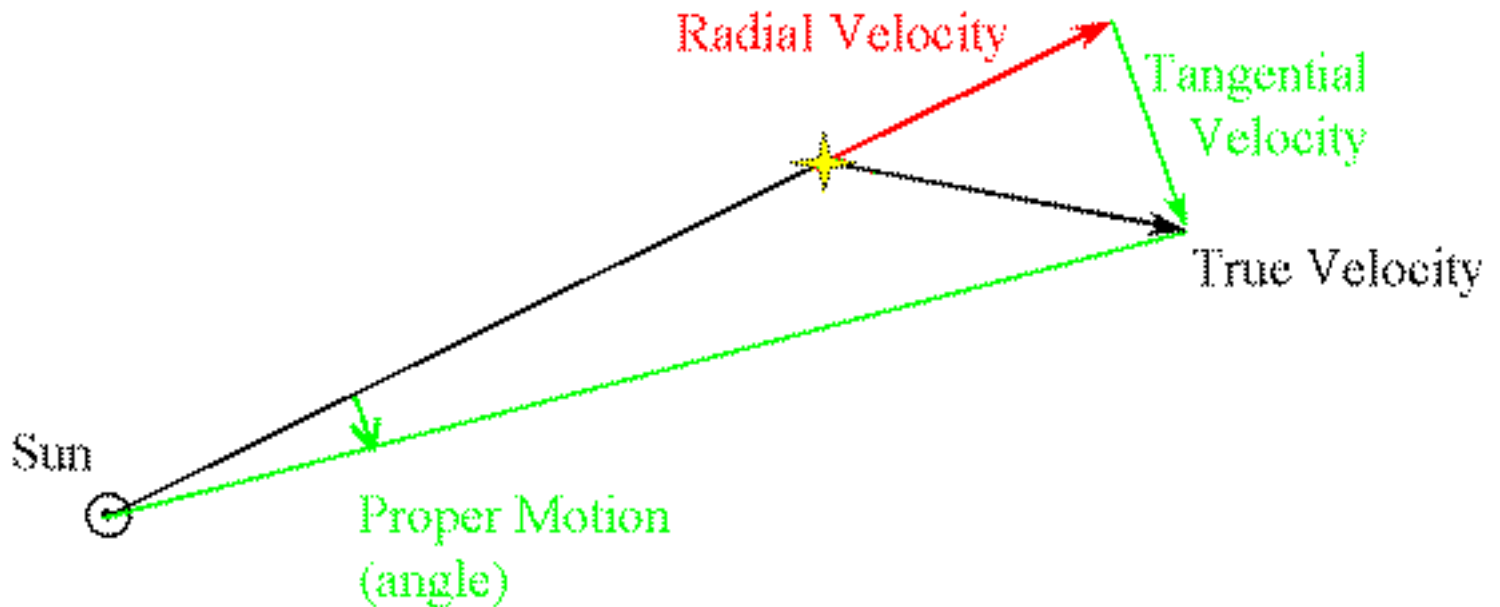
- ***Kinematics*: the study of motions of stars (in this case, in galaxies) without consideration of how they acquired those motions.**
 - [Contrast with ***dynamics***, which concerns itself with the underlying physical interactions that give rise to observed motions and matter distributions]
- The goal is similar to the one we have when we observe the distribution of light: characterize the distribution of galactic content (stars, gas, dark matter) in phase space.

Measuring Motions

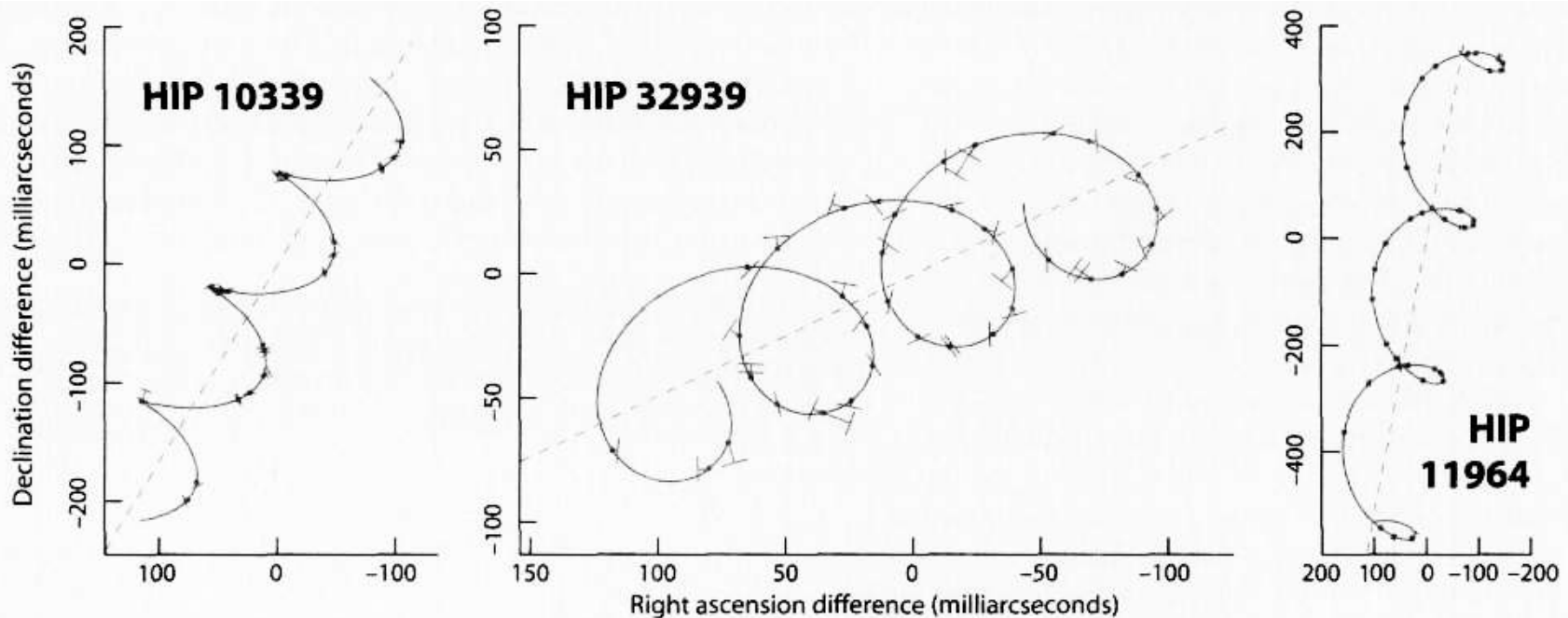
- Proper motions
- Radial velocities from spectra
- Motions of gas (H I or CO); see Lecture 3

Proper motion measurements

Typical proper motion is ~ 0.1 arcsec/year.
Largest: 10.25 arcsec/yr (Barnard's Star).



Hipparcos: PM+Parallax



The apparent paths of three stars across the sky during the three years of the Hipparcos mission. Each looping line shows the combination of parallax (an ellipse) and proper motion (a straight line) that best fits the data. The star's measured positions are shown by T-like intersections; these are often hidden under the dots, which mark their best-fit places on the line. Each curlicue in the 118,000-star database is different. From the Hipparcos Intermediate Data Web page.

Proper Motion Surveys: Space

“Industrial” measurements of proper motions require time (patience). Or money (space missions).

Hipparcos (1989-1993):

- 118,200 primary catalog
- >2million (Tycho catalog)
- 0.6-1.0 mas precision

Successor: **Gaia (now)**

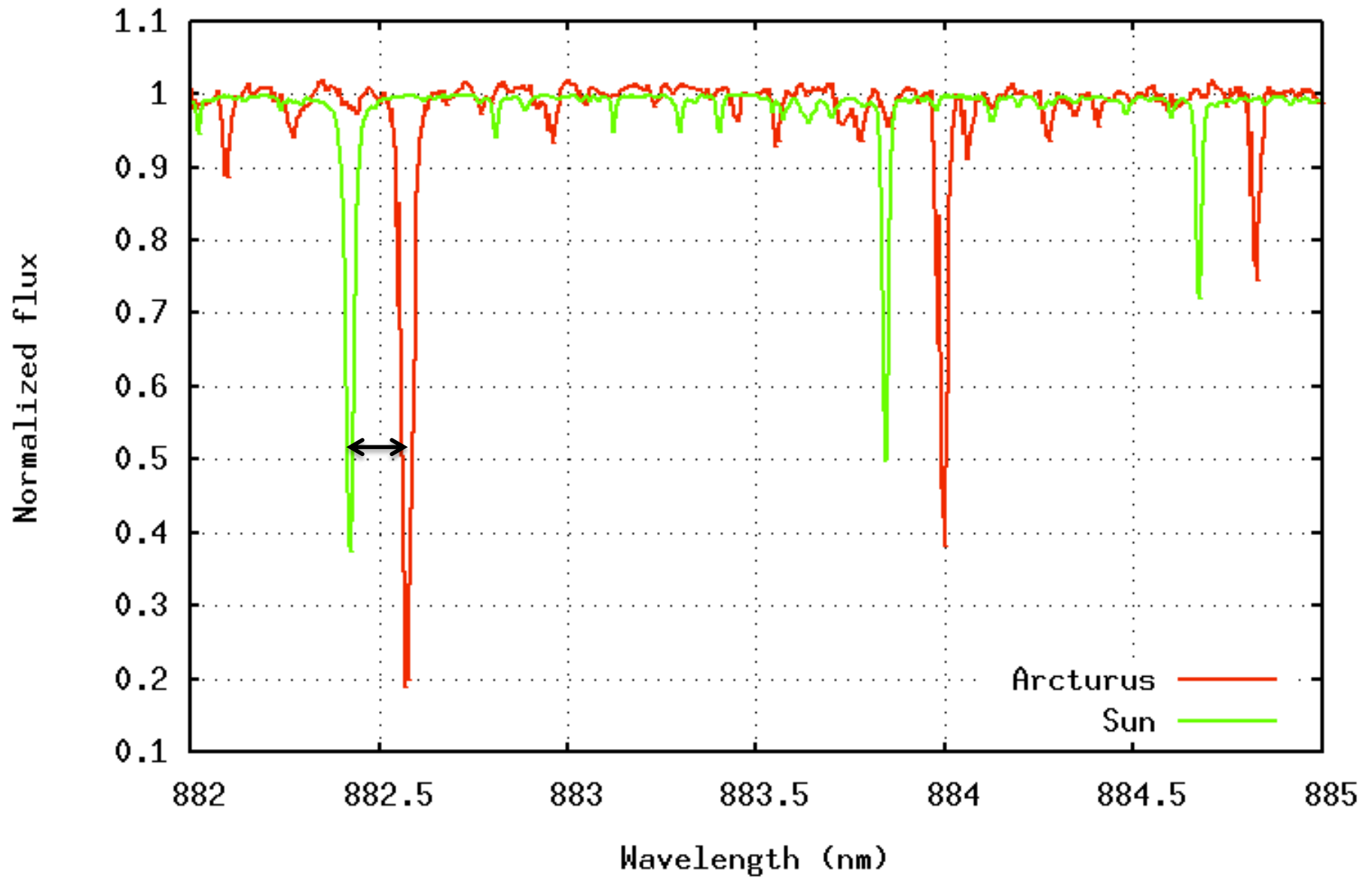
- 1.4 billion stars (and counting)
- 7-300 micro-arcsec precision



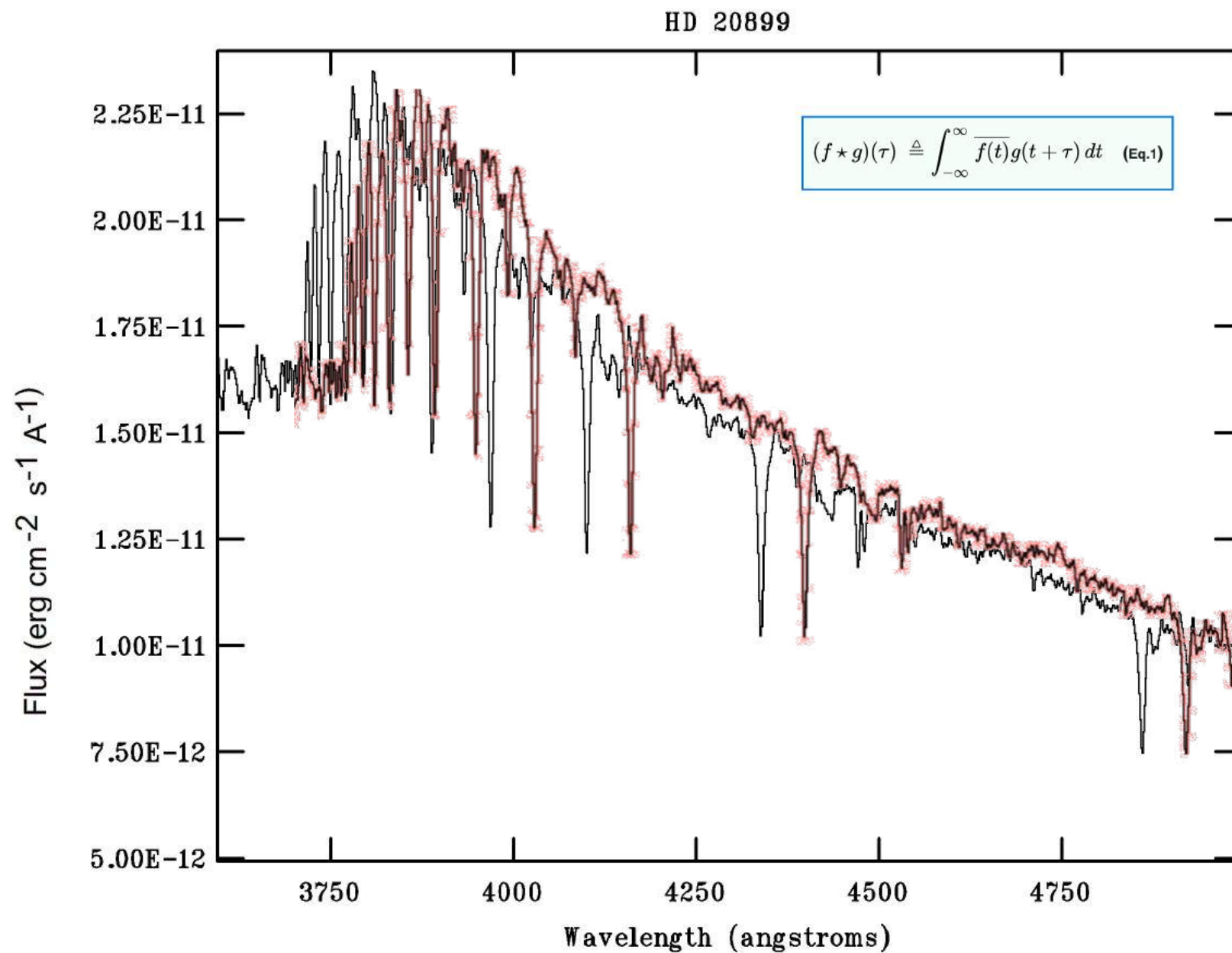
Spectroscopic Measurements of Radial Velocity

- Radial velocities are estimated from observing Doppler shifts in spectral lines
- Method:
 1. Acquire (high-res) spectra of objects of interest
 2. Identify spectral lines with known wavelengths
 3. Measure their Doppler shifts
 4. Estimate the velocity

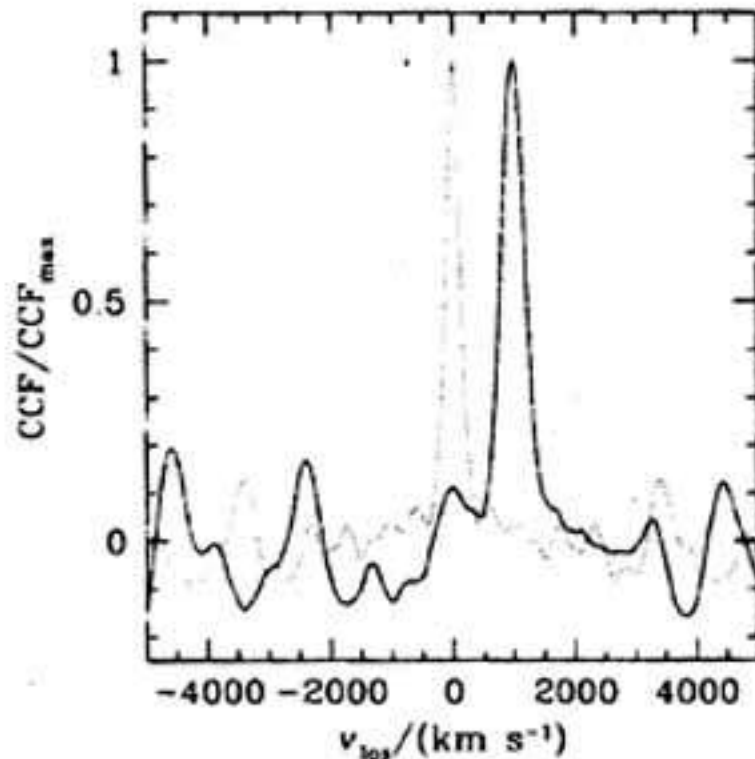
A tiny portion of the spectrum in the near-IR



Better: Cross-correlation with template spectra



Cross-correlation RV estimates



Compute the stellar cross-correlation function (CCF) and search for peaks.

Left: Cross-correlation function with a peak at ~ 1000 km/s

Figure 11.3 The cross-correlation function between the galaxy and star spectra shown in Figure 11.1. The dotted line shows the auto-correlation function of the star. The functions have been normalized by their peak values.

Some Sources of (stellar) RV Data

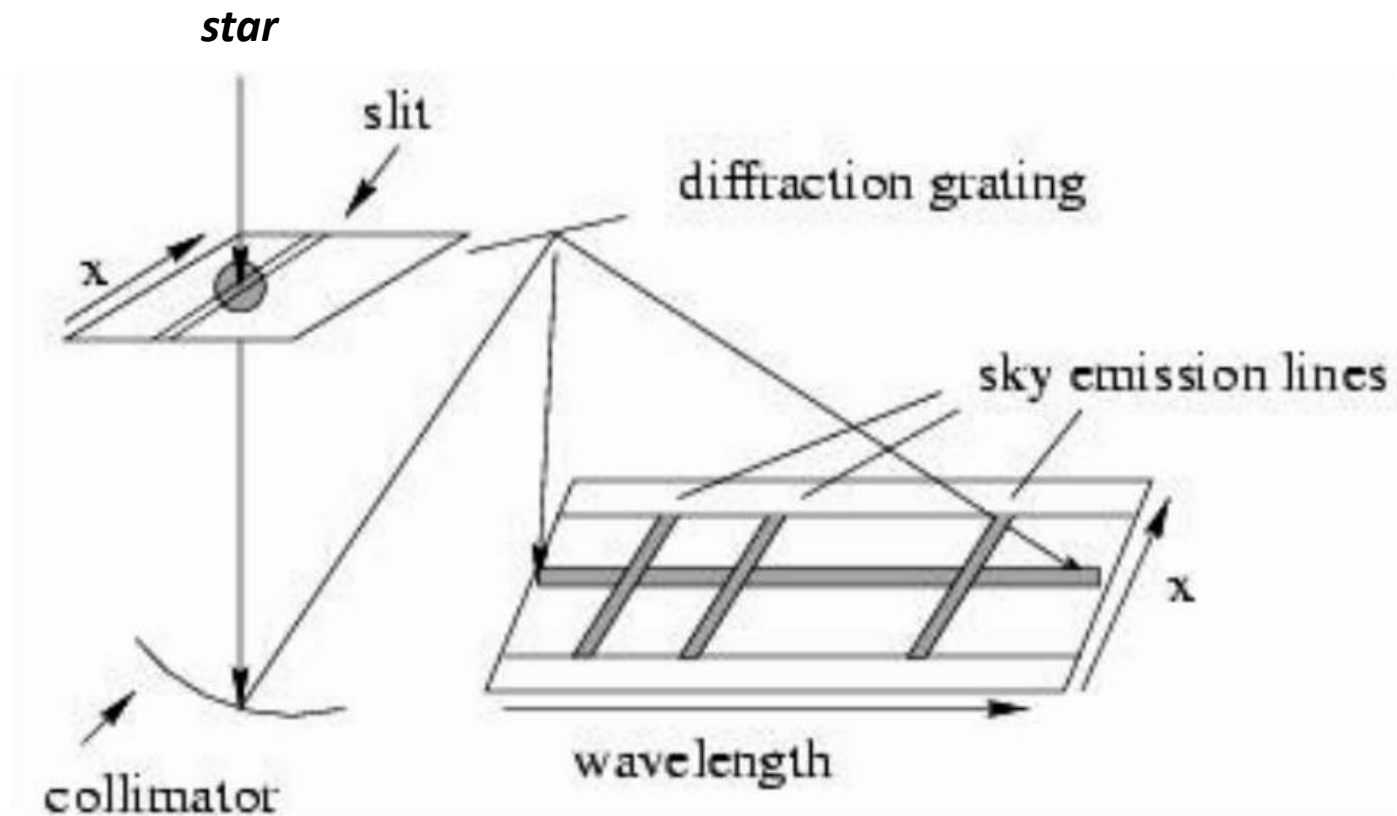
- **RAdial Velocity Experiment (RAVE) Survey**
 - <https://www.rave-survey.org/>
 - ~500,000 spectra (optical)
- **SDSS**
 - <http://sdss.org>
 - SEGUE: 400,000 stars (4 km/s)
 - BOSS: 250,000 stars
 - SDSS APOGEE: ~150,000 high-resolution IR spectra
- **GAIA**
 - <http://sci.esa.int/gaia/>
 - All stars to ~17th magnitude

Studying kinematics outside of the Local Group

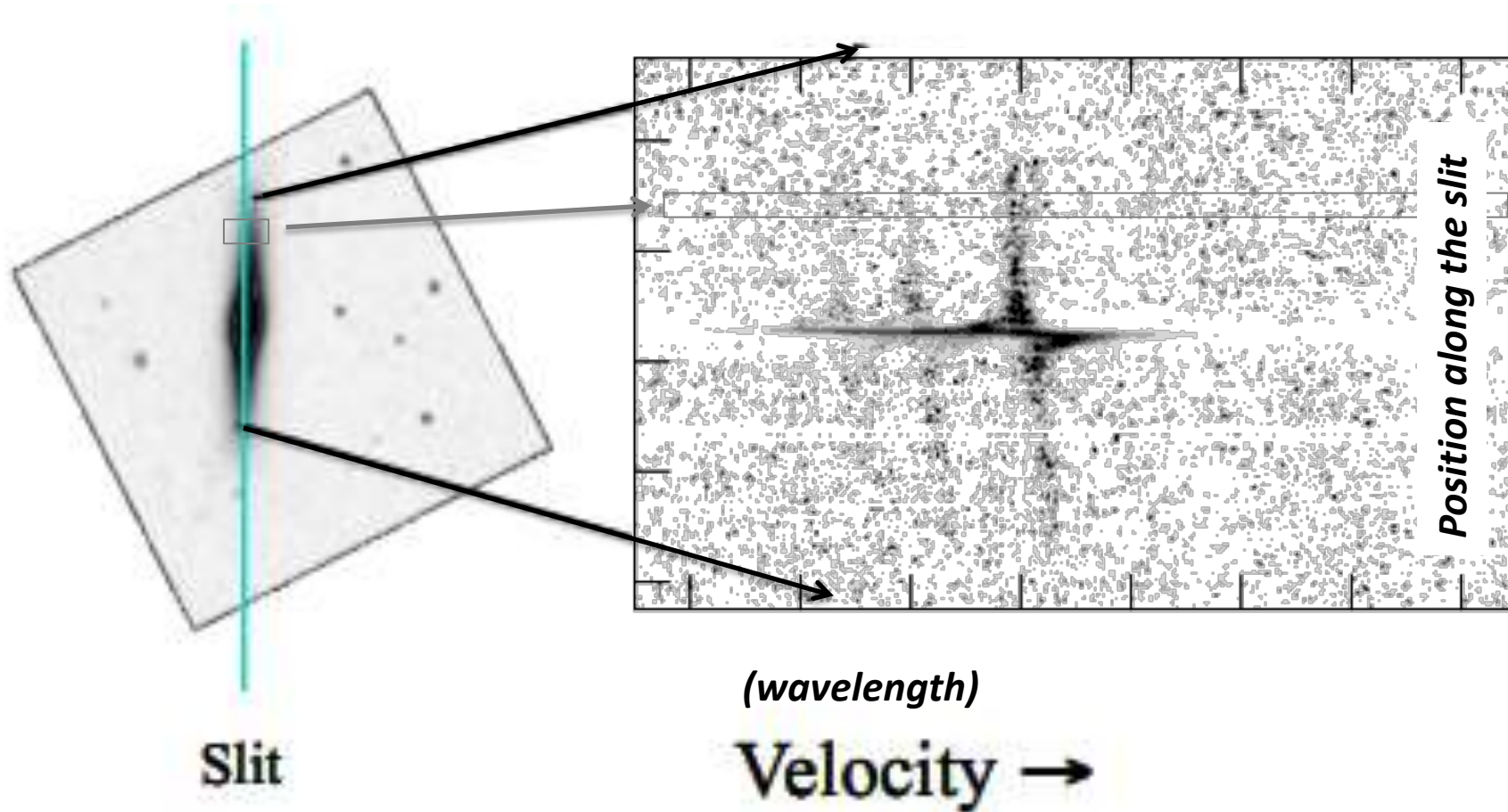
- Proper motions are too small to be measured beyond the Magellanic Clouds (maybe M31)
- Individual stars are (generally) not possible to resolve beyond the Local Group
- We rely on radial velocities measured from spectroscopy

How are spectra acquired

- Slit spectra

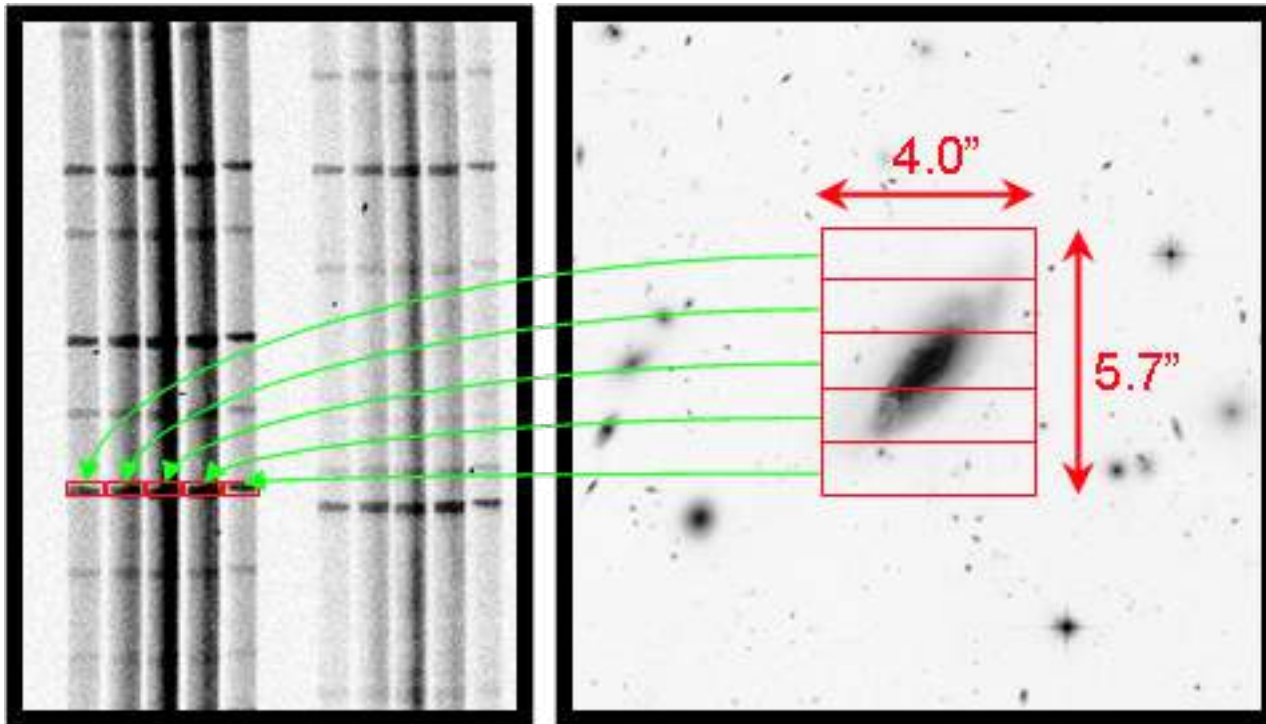


Long-slit spectroscopy of galaxies



(Nuclear region of M84; Bower et al. 1998)

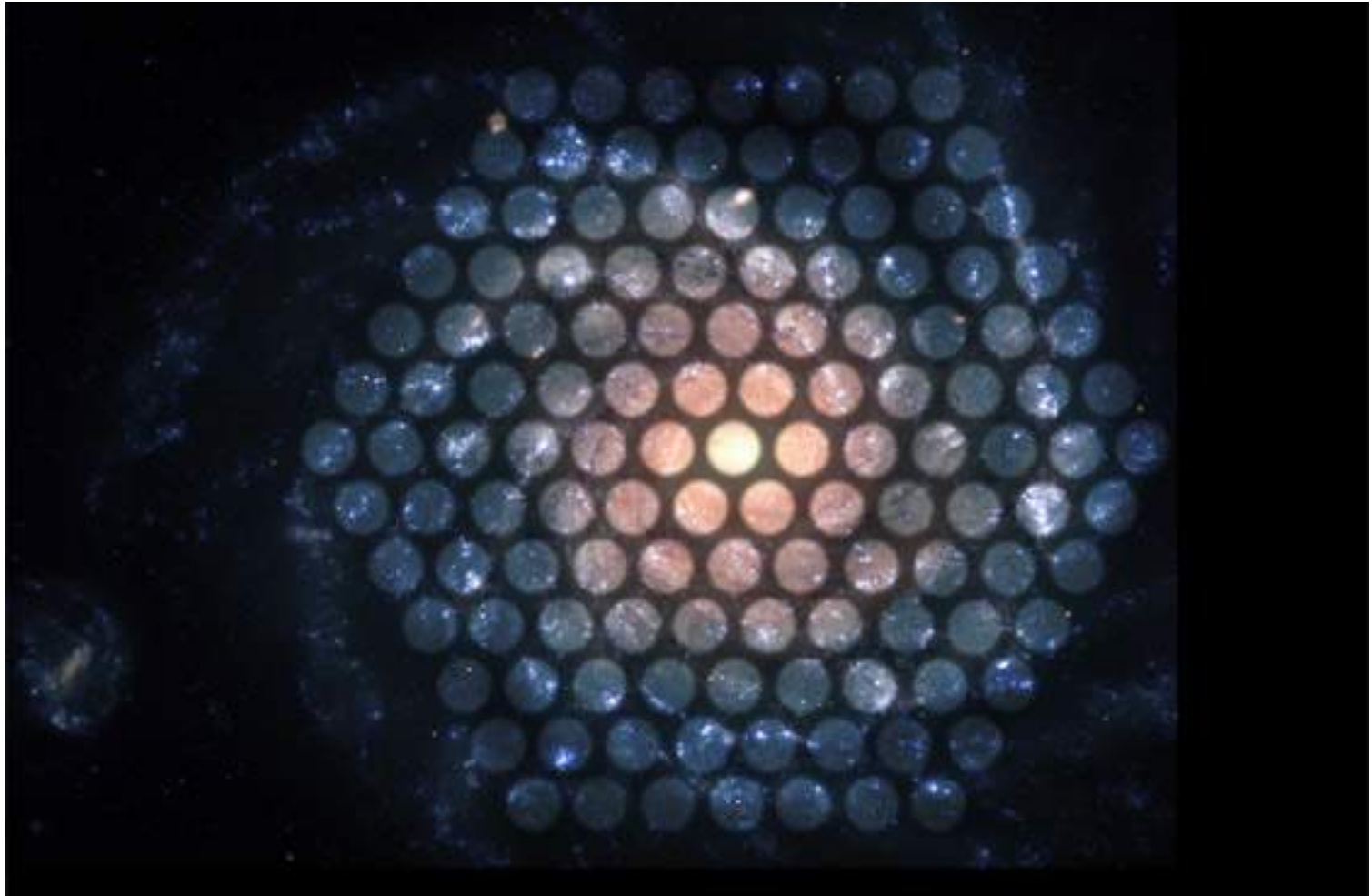
Going 2D: Integral Field Units



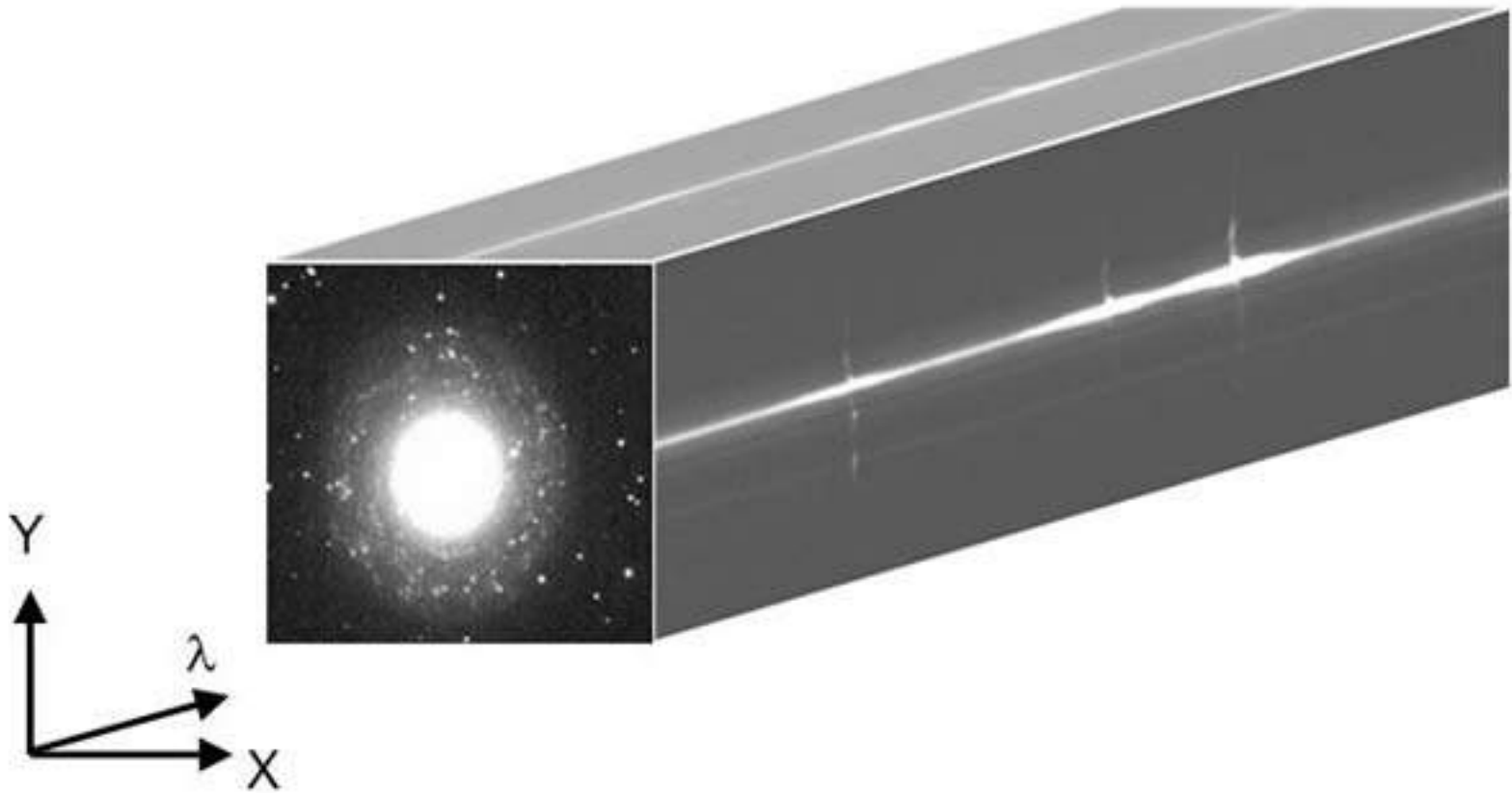
Wavelengths \rightarrow

From <http://www.eso.org/public/images/eso0426i/>

Fiber-fed IFUs



Datacube in (x, y, λ)



Interpreting the spectra

- The measured spectrum is a sum of (doppler shifted) spectra of all matter (stars, dust) along the line of sight.

How spectra from parts of the galaxy combine to create the effective spectrum



Note how the spectral lines in the spectrum of the galaxy – $G(\lambda)$ – are broader than the lines in the spectrum of the star, $S(\lambda)$.

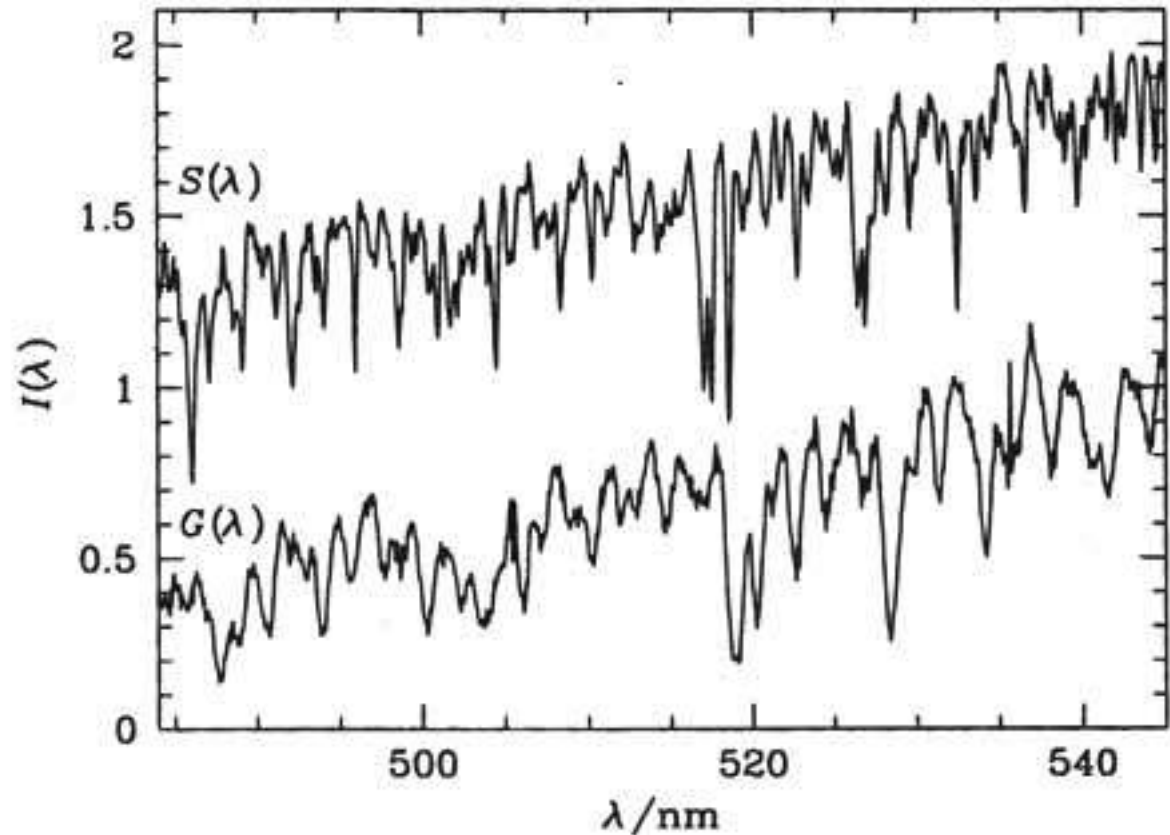
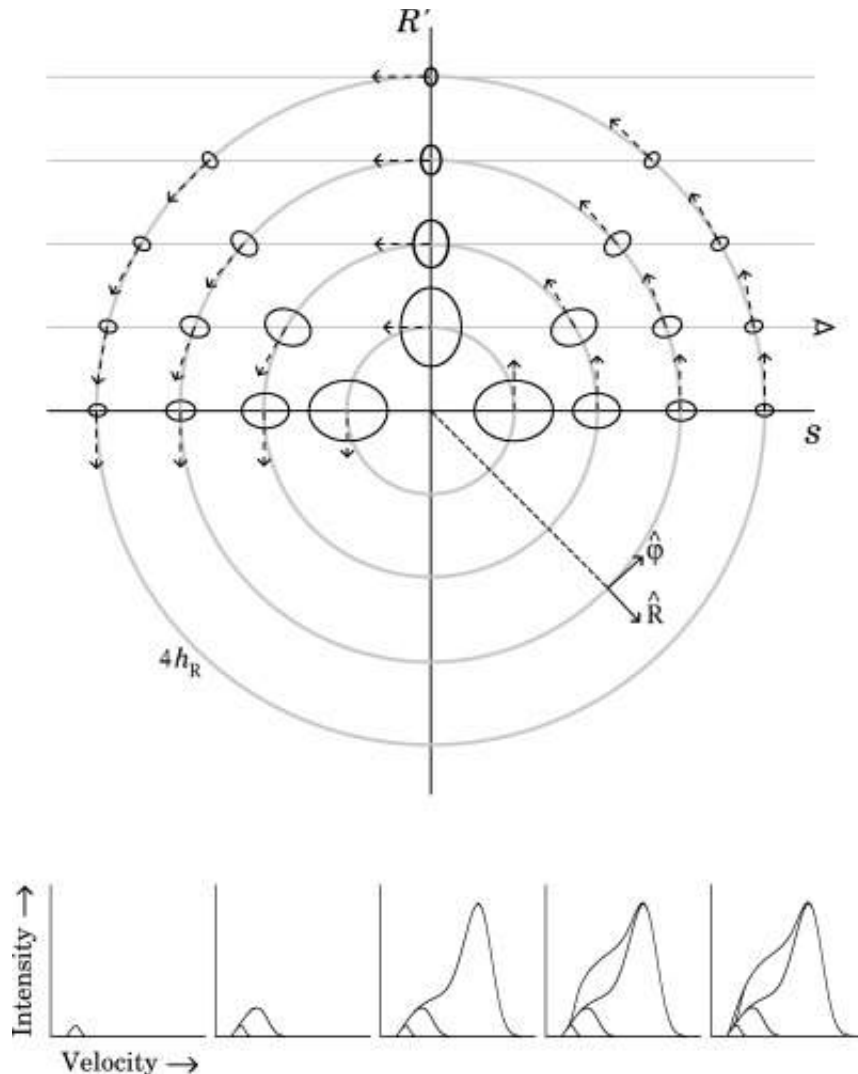


Figure 11.1 Spectra of a K0 giant star (S) and the center of the lenticular galaxy NGC 2549 (G). These data cover a small part of the optical spectrum around the strong Mg b absorption feature at 518 nm.

Line of Sight Velocity Distribution



Sketch of the galaxy plane illustrating the **build-up of the LOSVD** in an edge-on disc. Top, view of the disc plane. Circles mark galactocentric radii of 1–4 disc scale lengths. The horizontal lines represent sightlines crossing the receding side of the disc. The arrows and ellipses represent the stellar velocity and velocity dispersion, respectively. The symbol size indicates the amplitude of the rotation/dispersion.

Bottom, LOSVD build-up along the line of sight as marked by the eye in the top panel, from far behind the line of nodes (left) to the near side (right).

Characterizing the LOSVD

- Except for the highest quality (resolution, SNR) data, it's very difficult to directly reconstruct the full LOSVD in a parameter-free fashion.
- Instead, we adopt *models* (Gaussian, moment expansions, Gauss-Hermite series, etc.) for the shape of the LOSVD and fit their parameters:
 - Systemic velocity
 - Velocity
 - Dispersion
 - Higher-order moments (skewness, kurtosis, ...)

Determining v_{los} and σ by cross-correlating with a template

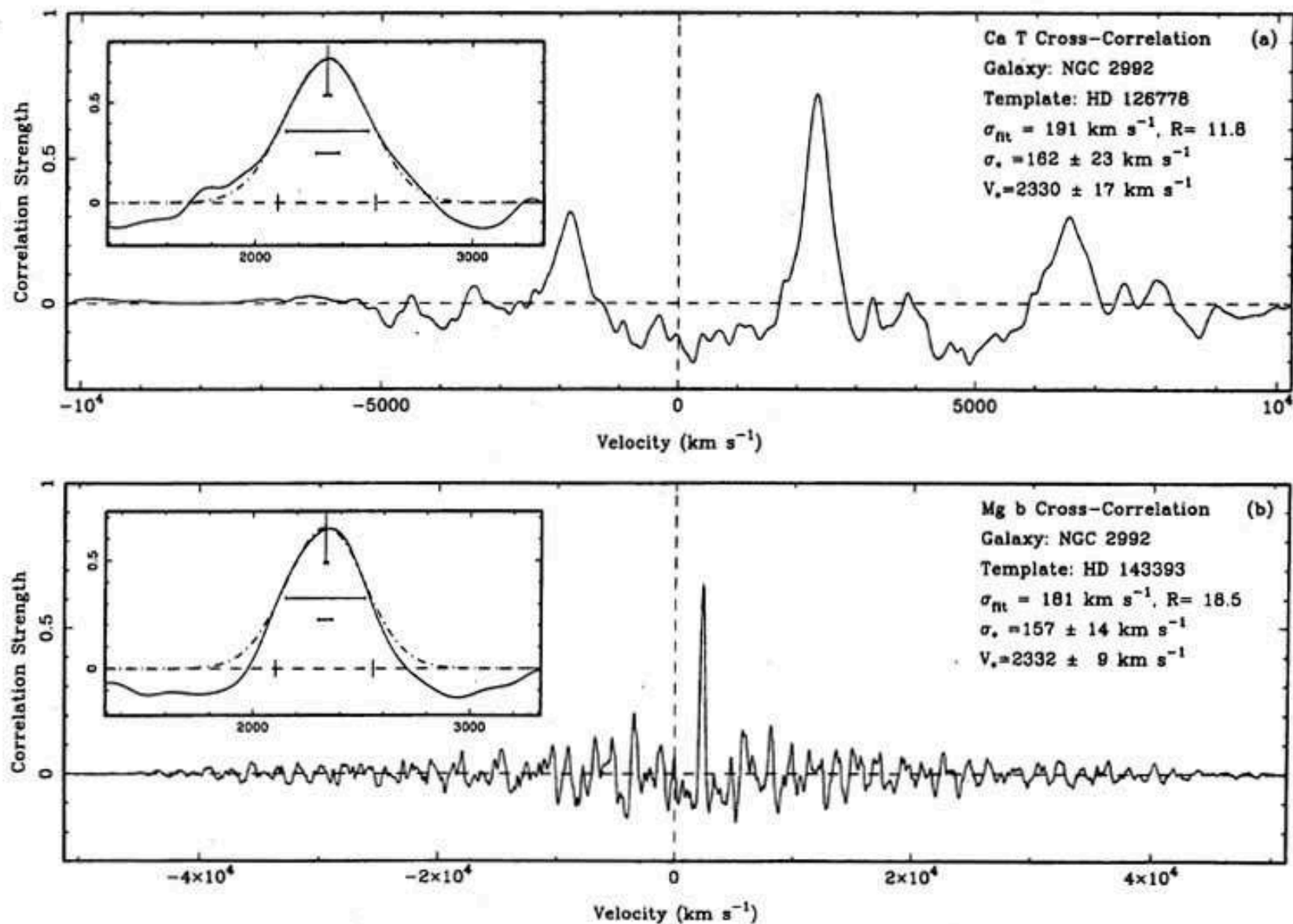


FIG. 4.—Cross-correlation functions for NGC 2992 are displayed in each spectral range to show differences in the two spectral regions. The insets show expansion of the area near the peak. The dash-dot line is the Gaussian fit, with the peak center and error marked as the vertical line and error bar. Below this, two horizontal bars are drawn to represent the resolution-corrected velocity width and its error. The tick marks on the dashed $Y = 0$ line show the region fitted.

Beyond v_{los} and σ :

Right: The shape of the LOSVD when varying higher-order parameters in the truncated Gauss-Hermite series expansion

BM'98

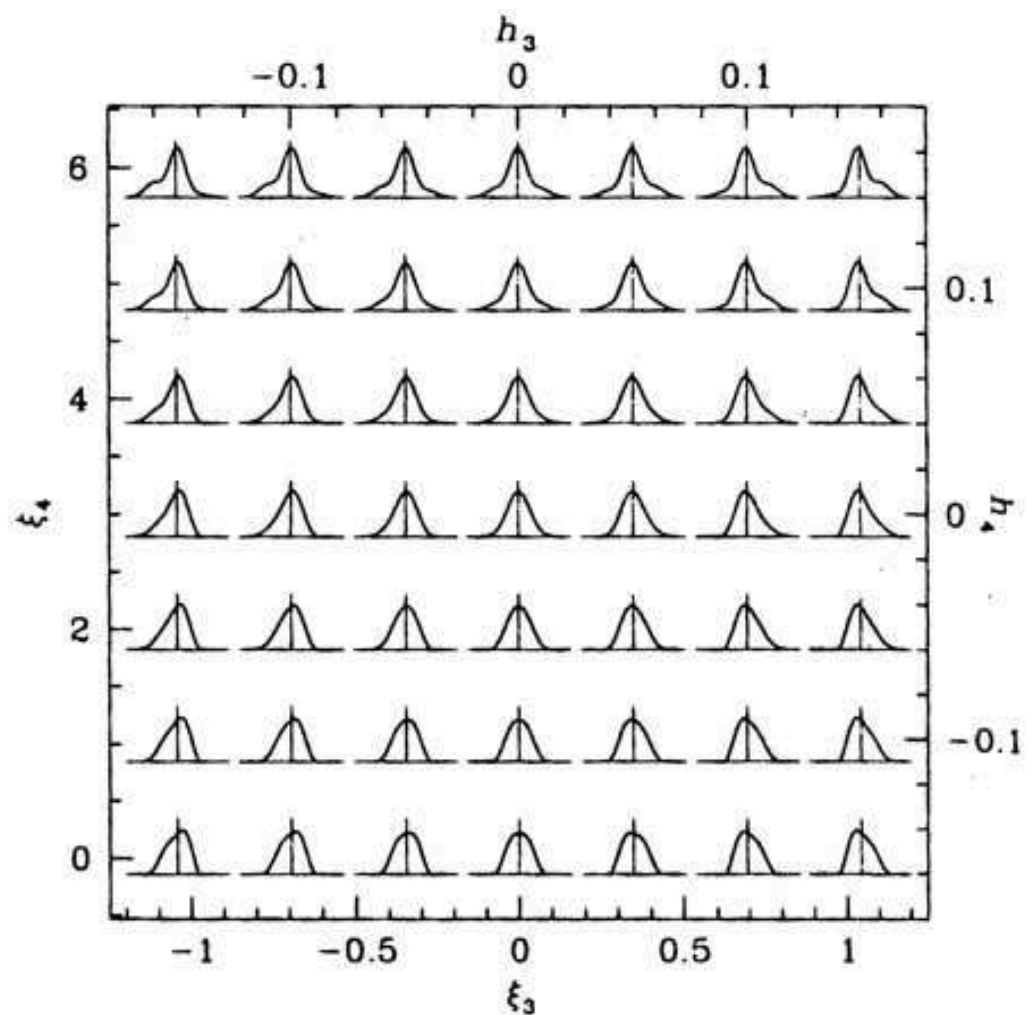
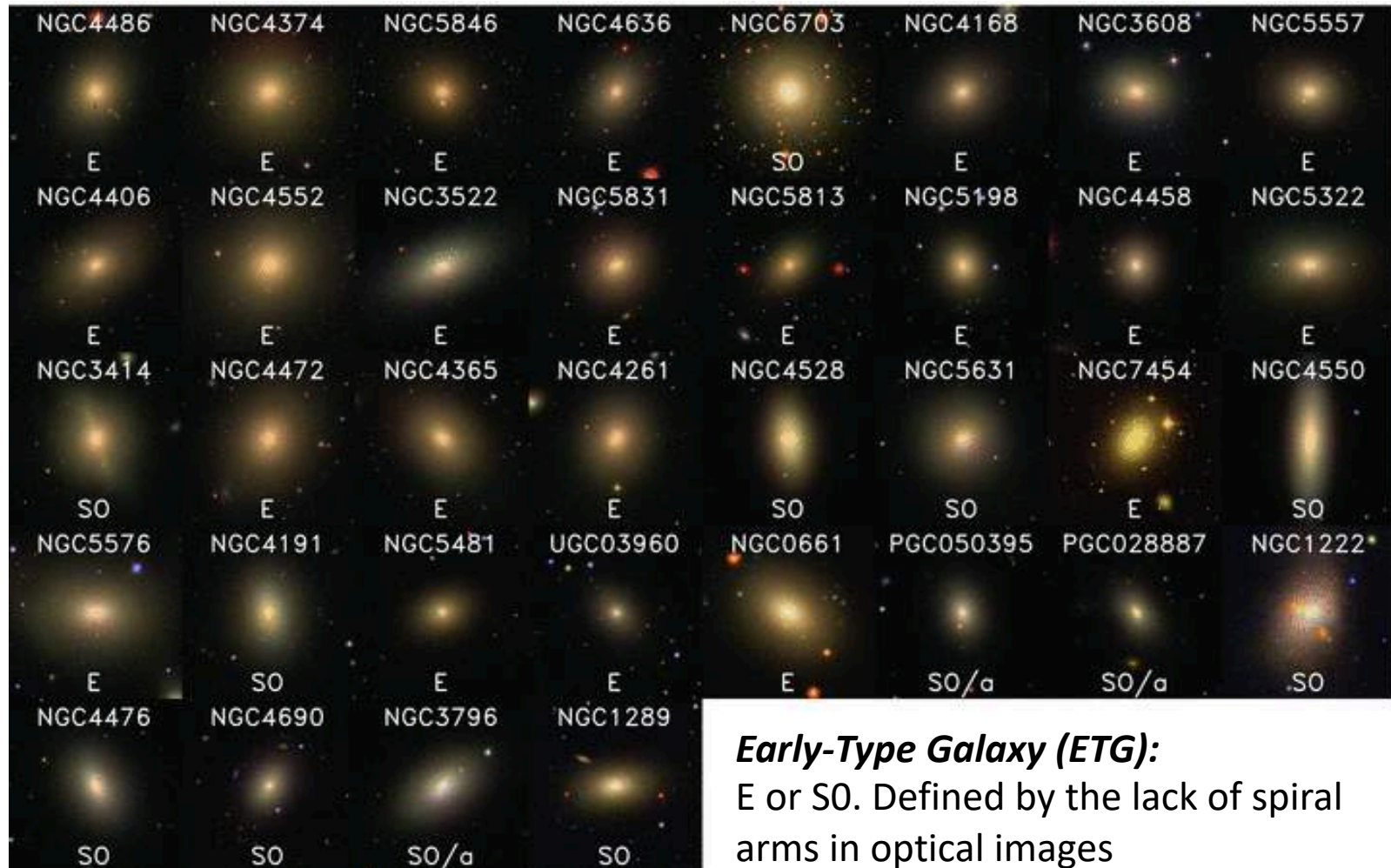


Figure 11.5 Montage showing how a velocity distribution typically changes depending on its shape parameters ξ_3 and ξ_4 . The central distribution is a pure Gaussian ($\xi_3 = 0$, $\xi_4 = 3$). All distributions have identical values for the Gauss-Hermite parameters \bar{v}_{los} (marked as the y-axis for each LOSVD) and σ_{los} . The right-hand and top axes are marked with the approximately corresponding values of the quantities h_3 and h_4 that are defined by equation (11.12).

Using Kinematics to Learn about Galaxies

Observations: Early Type Galaxies



ETG: Faber Jackson

- Faber & Jackson (1976)
- Empirical power-law relation between the luminosity and the central stellar velocity dispersion of elliptical galaxies:

$$L \propto \sigma^4$$

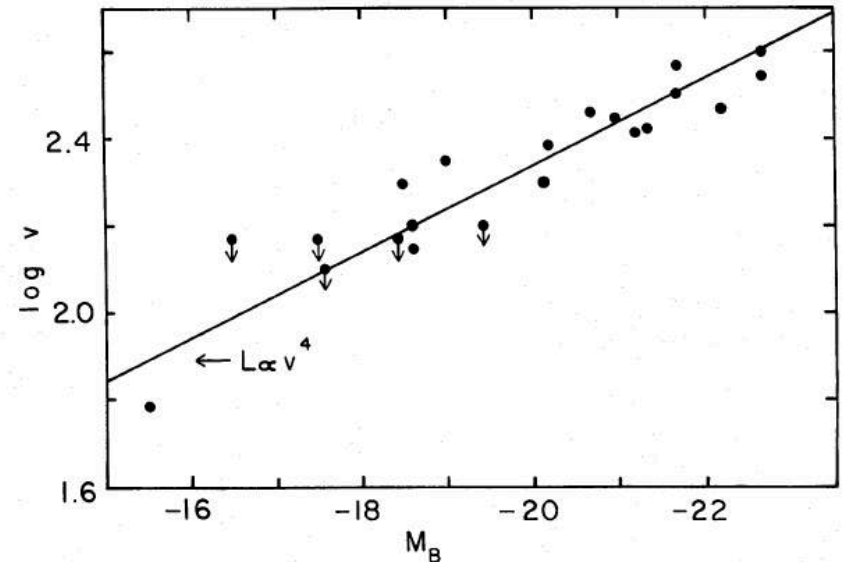


FIG. 16.—Line-of-sight velocity dispersions versus absolute magnitude from Table 1. The point with smallest velocity corresponds to M32, for which the velocity dispersion (60 km s^{-1}) was taken from Richstone and Sargent (1972).

Faber and Jackson (1976)

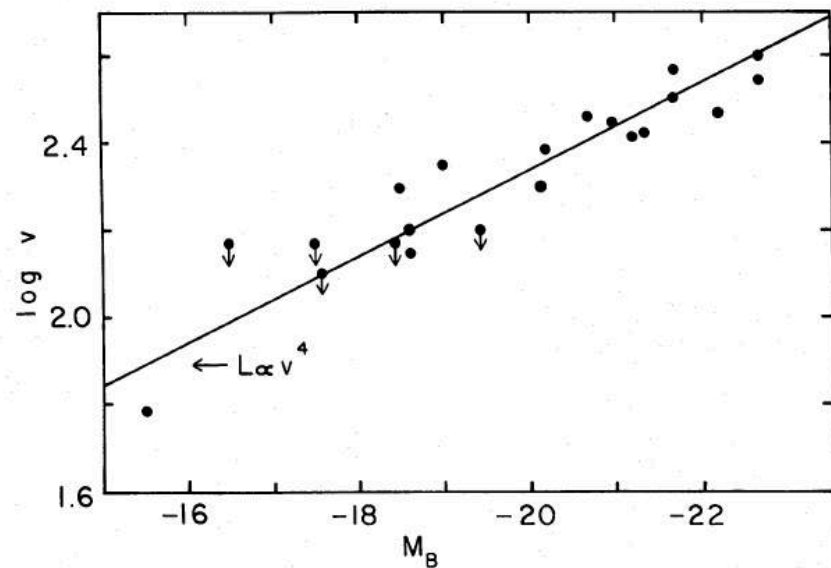
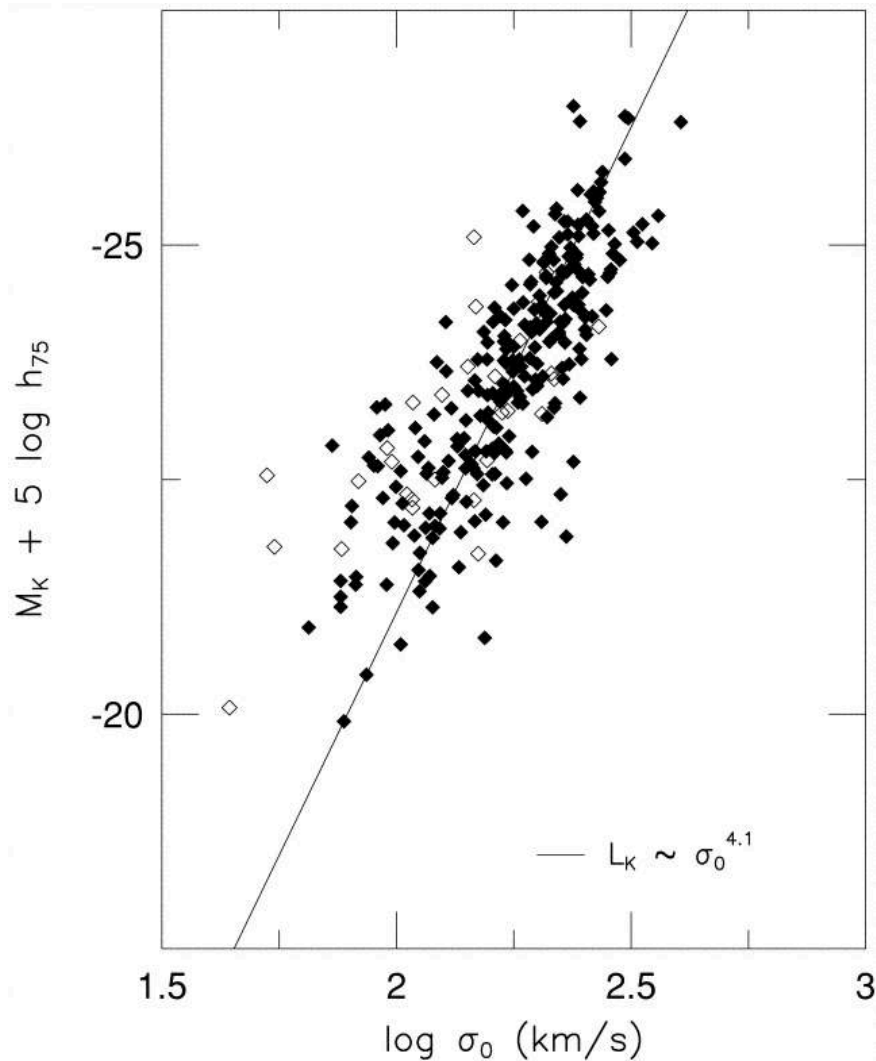


FIG. 16.—Line-of-sight velocity dispersions versus absolute magnitude from Table 1. The point with smallest velocity corresponds to M32, for which the velocity dispersion (60 km s^{-1}) was taken from Richstone and Sargent (1972).

Kormendy and Djorgovski (1989) ARA+A 27, 235



The Physics Behind F-J Relation

- Faber-Jackson relation can be theoretically explained under the following assumptions:
 1. Ellipticals are, virialized, gravitationally bound systems
 2. Their mass-to-light ratios are constant and the same across all galaxies
 3. Their surface brightnesses are identical

Fundamental Plane

One of our previous assumptions is less borne out by the data than the others: not all ellipticals have the same surface brightness.

This is likely (among other things) due to slightly different formation scenarios/histories.

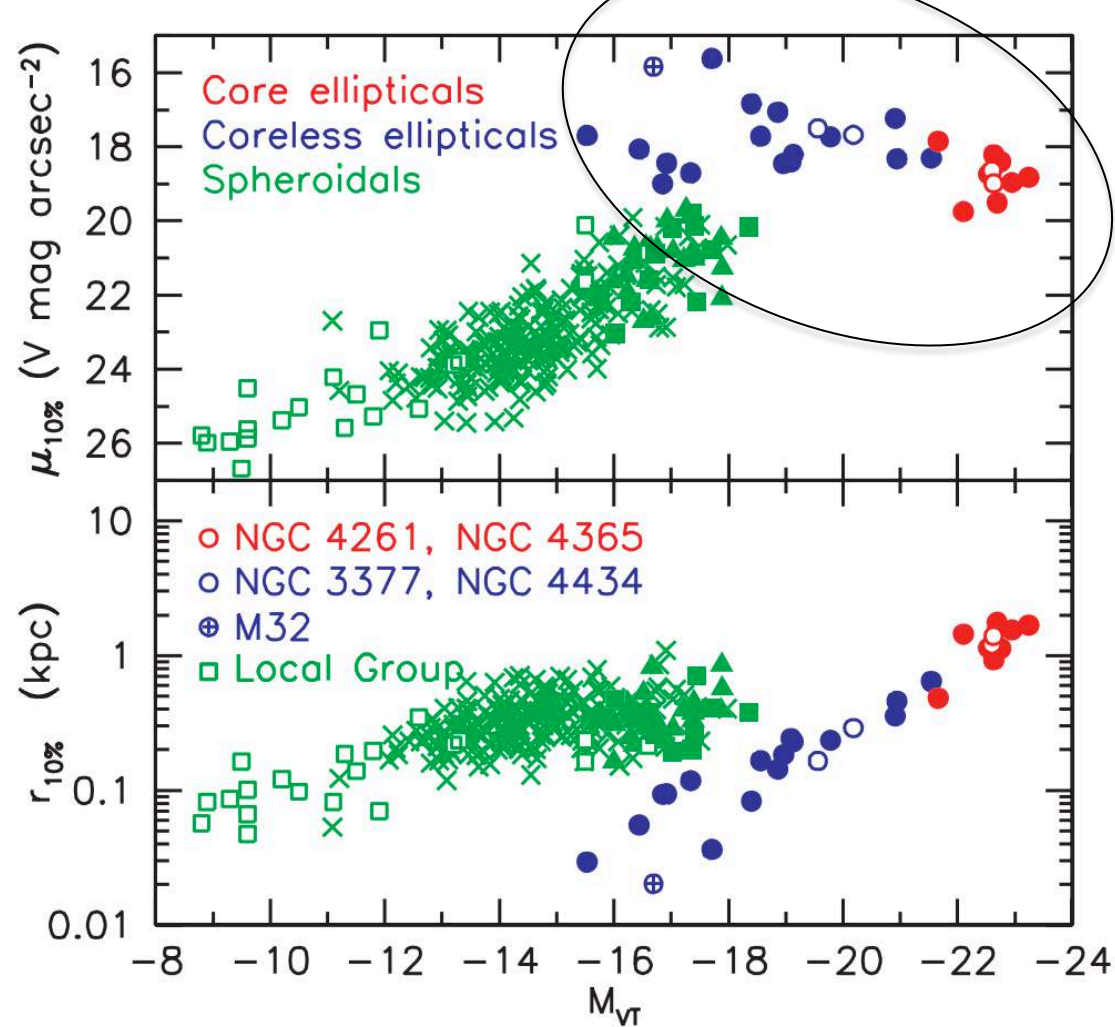


Figure 34. “Central” parameter correlations for the main bodies of elliptical and spheroidal galaxies. Here $r_{10\%}$ is the major-axis radius of the elliptical isophote that contains 10% of the light of the galaxy and $\mu_{10\%}$ is the surface brightness at that radius corrected for Galactic extinction. The 10%-light radius is approximately the smallest radius that is outside the nucleus in Sph galaxies and outside cores and extra light in Es. The center panel shows $\mu_{10\%}$ vs. total V-band absolute magnitude M_{VT} . The bottom panel shows $r_{10\%}$ vs. M_{VT} . The symbols are as in Figure 33. The open squares are Local Group spheroidals from Mateo (1998) and McConnachie & Irwin (2006).

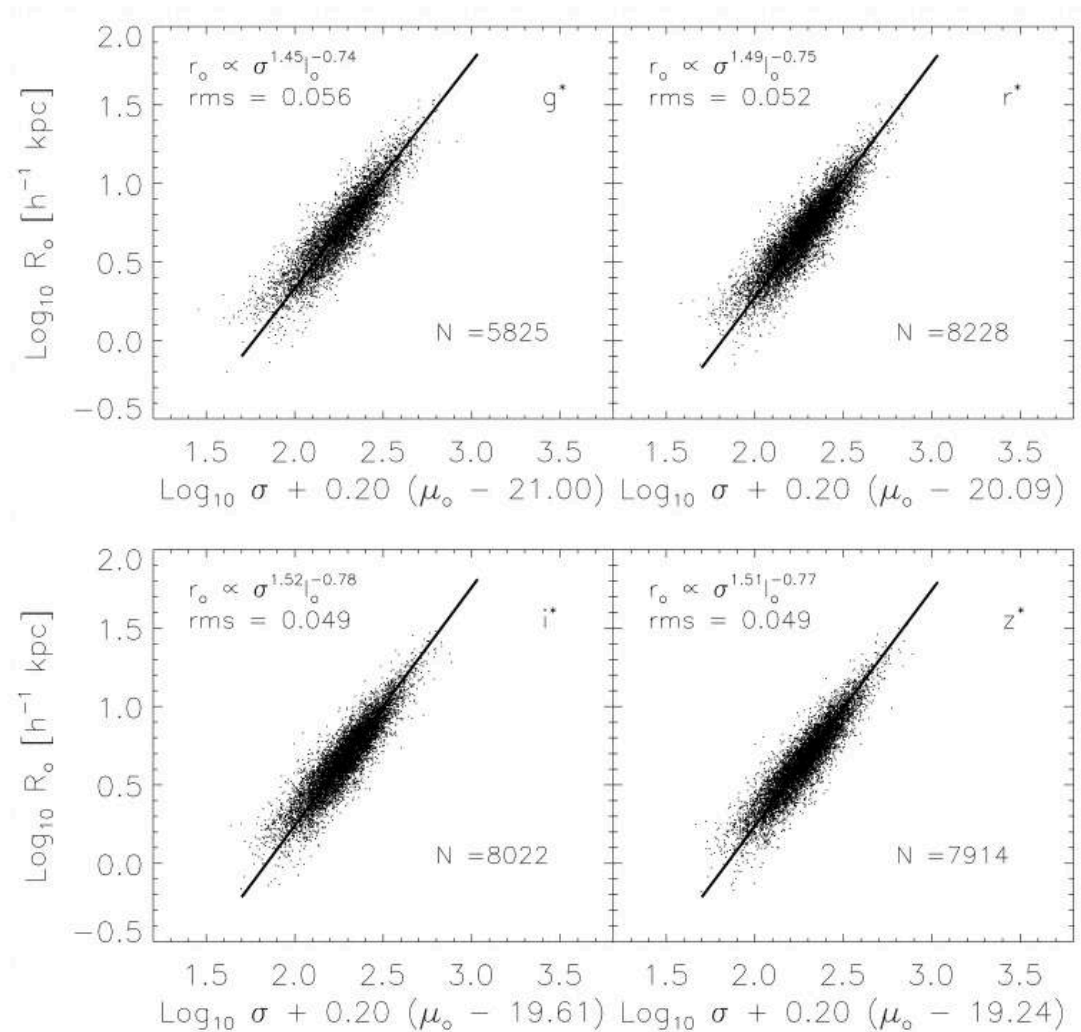
Fundamental Plane

One of our previous assumptions is less borne out by the data than the others: not all ellipticals have the same surface brightness.

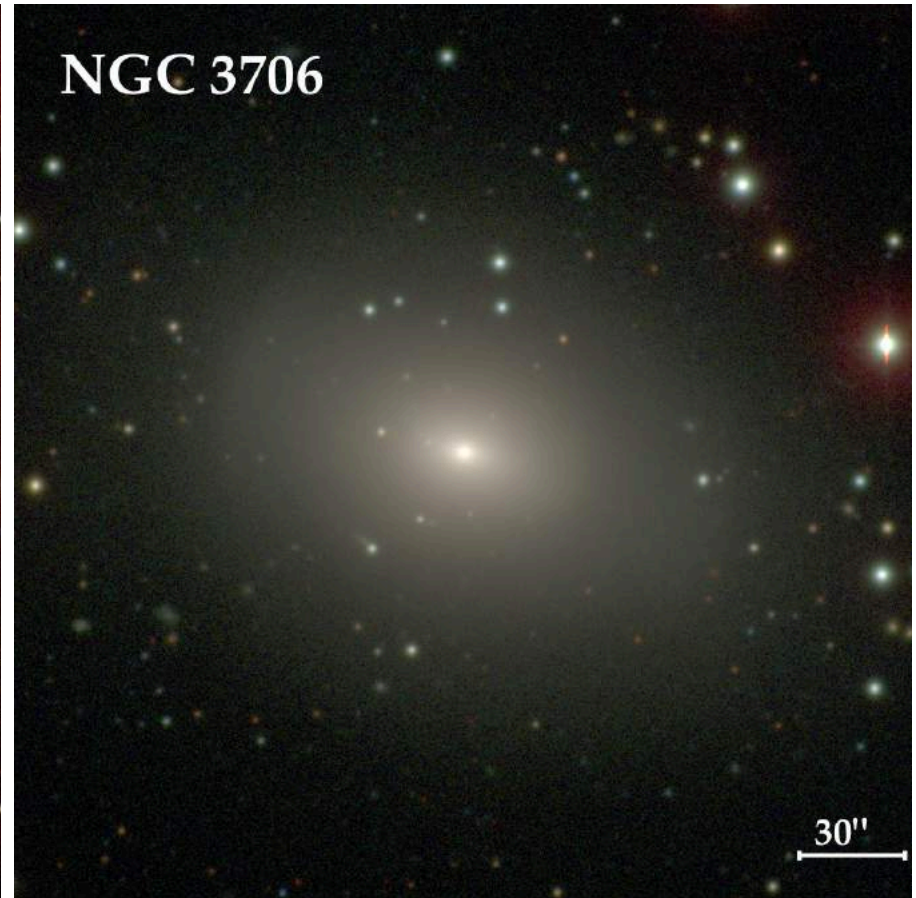
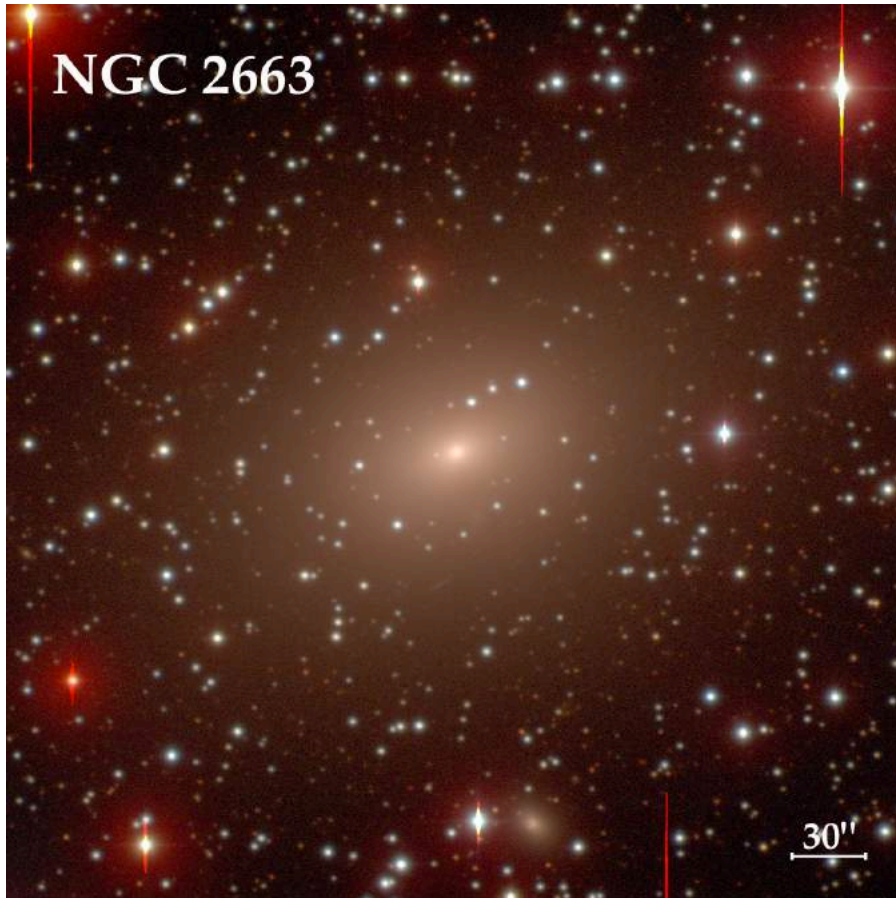
If we allow for a variable surface brightness (or radius) and fit:

$$L^\alpha * R^\beta * \sigma^\gamma = \text{const.}$$

we obtain a tighter relation.
This is the **Fundamental Plane** of Djorgovski and David (1979).



Are All Ellipticals the Same?



ETG: Do Ellipticals Rotate?

- They're not all the same! For example:
- Some exhibit very little (or no) signs of rotation (e.g., like NGC 2663), but most (~80%) do rotate (e.g., like NGC 3706).
- Today we identify the classes as “slow rotators” and “fast rotators”

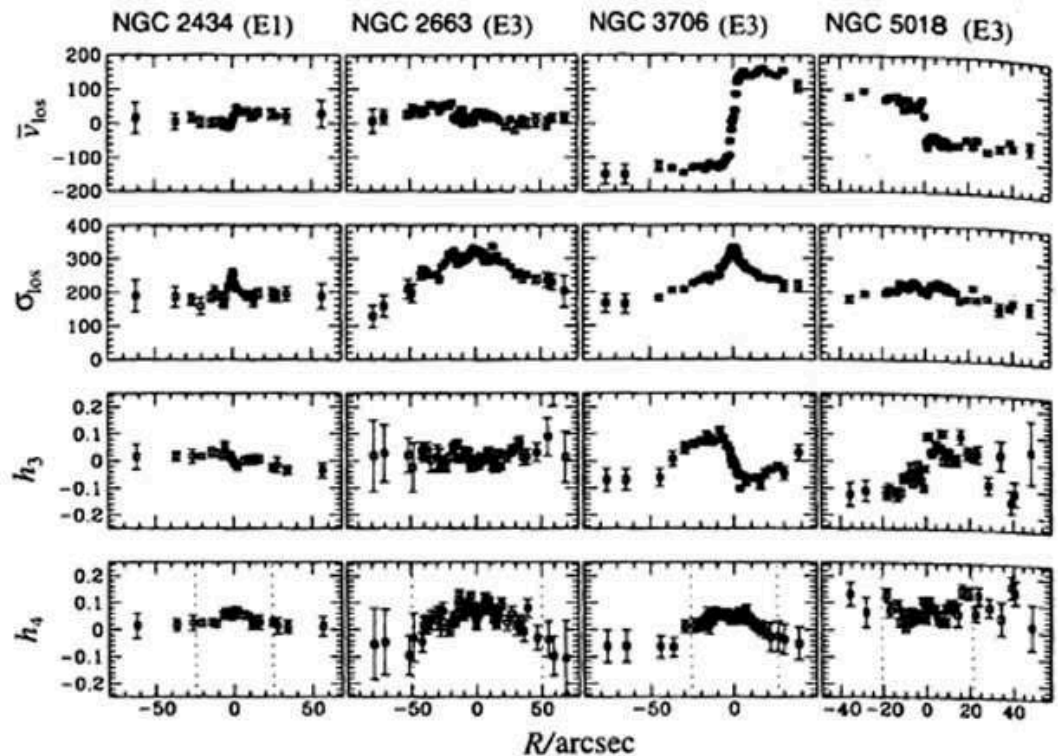
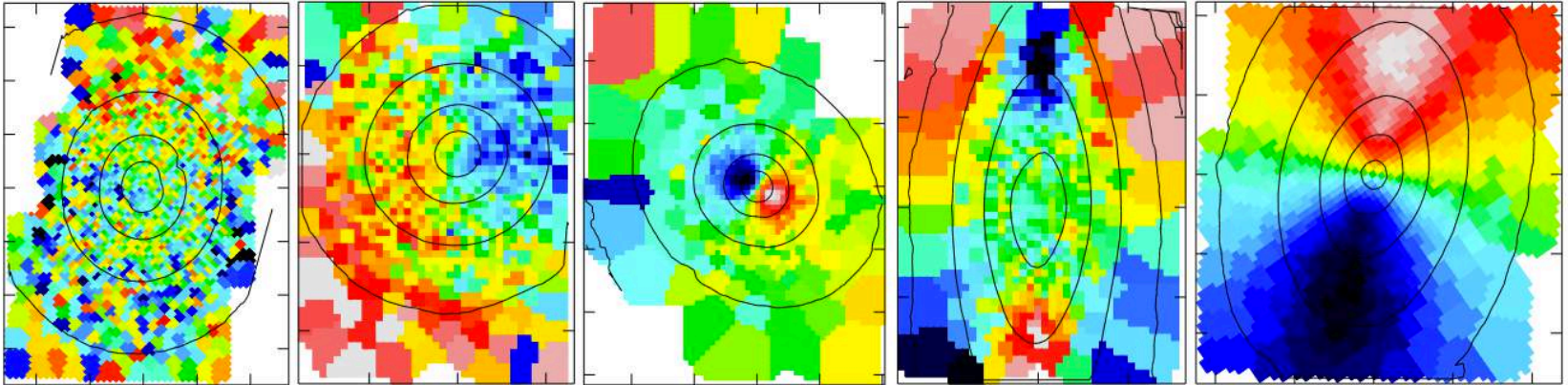


Figure 11.6 The large-scale major-axis kinematics for a sample of four giant elliptical galaxies. The LOSVDs of these systems have been parameterized using the truncated Gauss-Hermite expansion (§11.1.2). The dotted lines indicate the effective radius, R_e , for each galaxy. The Hubble classification (shown in parentheses) is based on the galaxy's average ellipticity outside $R_e/2$. [After Carollo *et al.* (1995)]

Interpret... These... Diagrams!



Line-of-sight velocity reconstructed for a series of galaxies from IFU observations.

Color map: the line of sight velocity (red – receding, blue – approaching the observer).

Contours: contours of constant surface brightness.

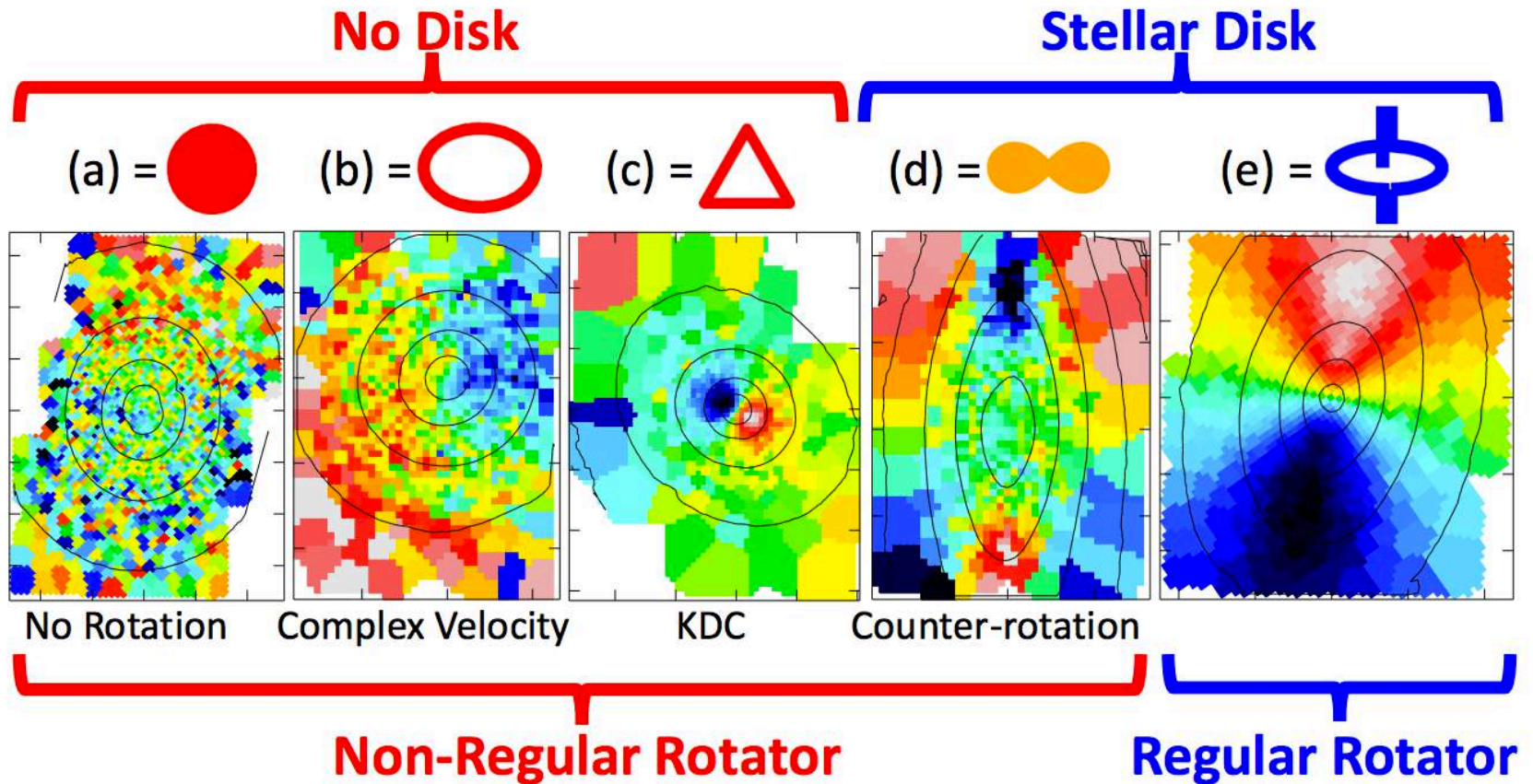


Figure 4

Morphological classification of stellar kinematic. The features in large samples of ETGs can all be qualitatively described by five classes. (a) No clearly detectable rotation (NGC 4374); (b) Clear but not regular rotation (NGC 4552); (c) kinematically distinct core (KDC; NGC 5813); (d) Counter rotating disks (NGC 4550); (e) Regular extended disk-like rotation (NGC 2974). The five classes were introduced by [Krajnović et al. \(2011\)](#). The Voronoi binned ([Cappellari & Copin 2003](#)) kinematics were taken from [Emsellem et al. \(2004\)](#). The symbols above the maps are used consistently throughout this review.

ETG Classes: fast/slow rotators

- ETGs exhibit some diversity, *but two main classes of ETGs can be separated using stellar kinematics: the fast and slow rotators.*
- The slow rotators are weakly triaxial and **dominate above $M_{\text{crit}} \approx 2 \times 10^{11} M_{\text{solar}}$**
- **Theorized formation mechanism:**
 - Fast rotators ETGs start as star forming disks and evolve through a channel dominated by gas accretion, bulge growth, and quenching (== cessation of star formation).
 - Slow rotators assemble near the center of massive halos via intense star formation at high redshift, and remain as such for the rest of their evolution via a channel dominated by gas poor mergers

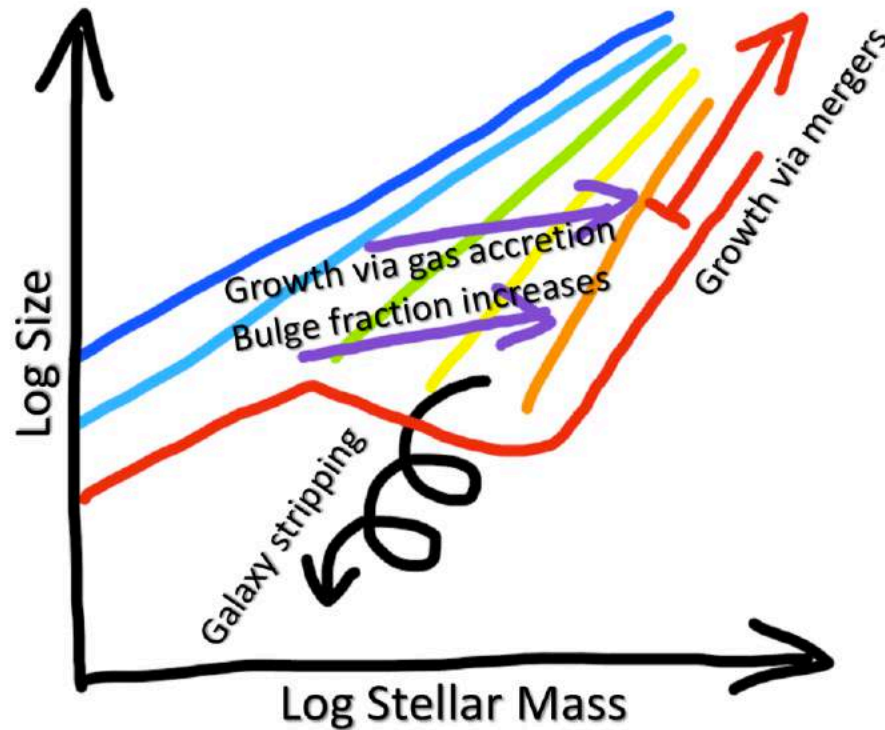


Figure 29

Galaxy evolution on the mass-size plane. Although the evolution of an individual galaxy is a complex combination of events, the observations indicate that the average evolution of ensembles of galaxies can be described by the following simple picture. The progenitors of fast rotators ETGs are star forming disks. They grow their mass, while slowly increasing their sizes, predominantly by gas accretion (purple lines). During this accretion they grow a bulge, which increases the likelihood for the galaxy to have its star formation quenched. They end up as bulge-dominated and passive fast rotators near the ZOE. Slow rotators build up most of their mass rapidly at high- z and subsequently grow mostly by gas poor (dry) merging, while varying their size nearly proportionally to their mass or more (red line). They end up in the top right of this diagram. The region below the ZOE is not empty: it includes ultra compact dwarfs (UCD), which are the likely cores of normal galaxies which had their envelopes stripped by the gravitational field of larger galaxies. (Based on fig. 15 of [Cappellari et al. 2013a](#) and fig. 28 of [van Dokkum et al. 2015](#))

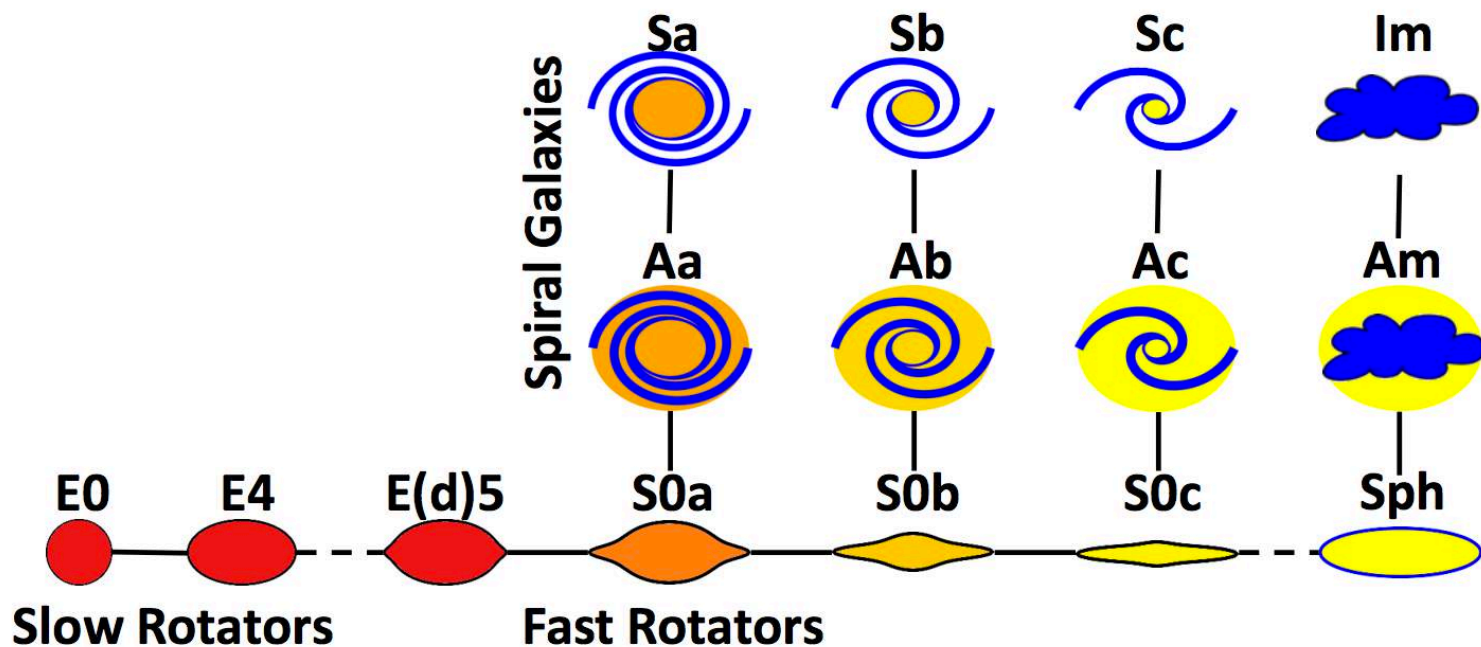
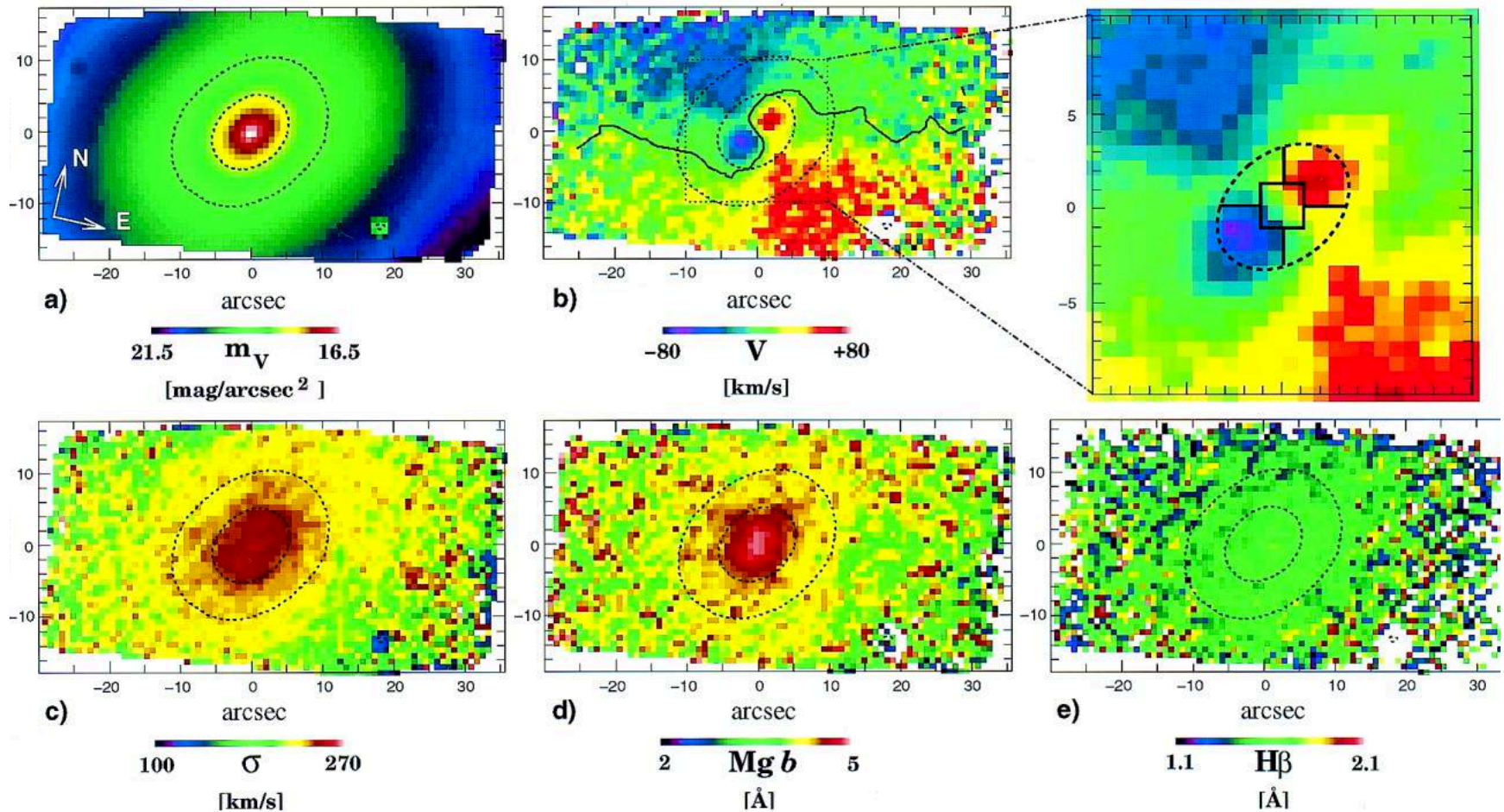


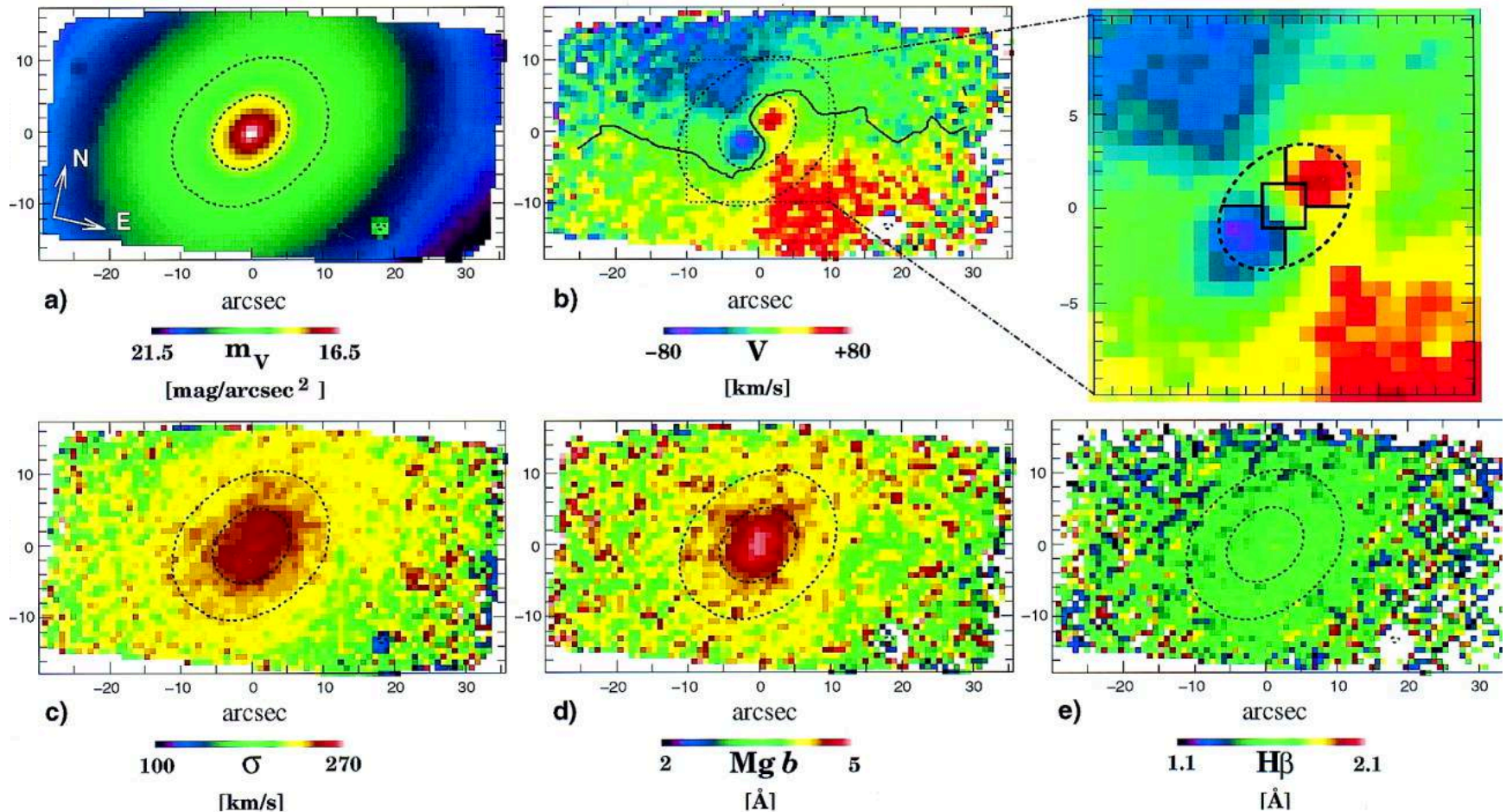
Figure 24

The “comb” morphology diagram. If all fast rotators could be seen edge-on, they would appear morphologically with a range of spheroid fractions ranging from thin S0s, to flat ellipticals with disky isophotes E(d) (Kormendy & Bender 1996), as here illustrated. The fast rotators ETGs form a parallel sequence to spiral galaxies as already emphasized, for the subset of S0 galaxies, by van den Bergh (1976), who proposed the above distinction into S0a–S0c. Fast rotators are intrinsically flatter than $\epsilon \gtrsim 0.4$ and span the same full range of shapes as spiral galaxies, including very thin disks. However very few Sa have spheroids as large as those of E(d) galaxies, indicating that bulges must grow in the transformation. The slow rotators are always rounder than $\epsilon \lesssim 0.4$ and have central cores in their surface brightness. On the right-hand side of the diagram we included spheroidal Sph galaxies, following Kormendy & Bender (2012). These are bulge-less dwarf galaxies, but are significantly rounder than S0c disks. The black solid lines connecting the galaxy images indicate an empirical continuity, while the dashed one emphasizes the dichotomy between the fast and slow rotator ETGs. (Adapted from Cappellari et al. 2011b, with the addition of Sph galaxies from Kormendy & Bender 2012).

Q: What's Wrong in this Picture?



ETG: Kinematically Decoupled Cores



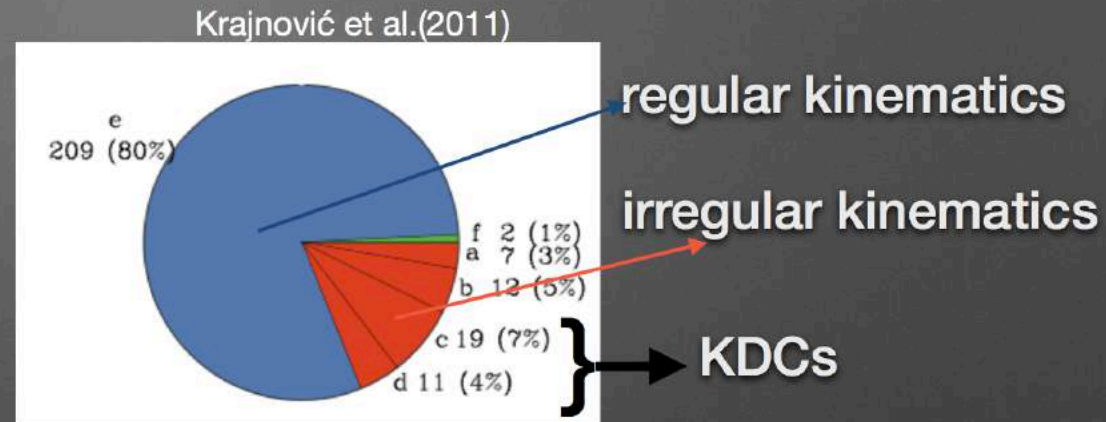
NGC 4365

The SAURON data clearly reveal the inner kinematic component, rotating around the photometric minor axis, as well as the outer kinematic component, rotating around the photometric major axis.

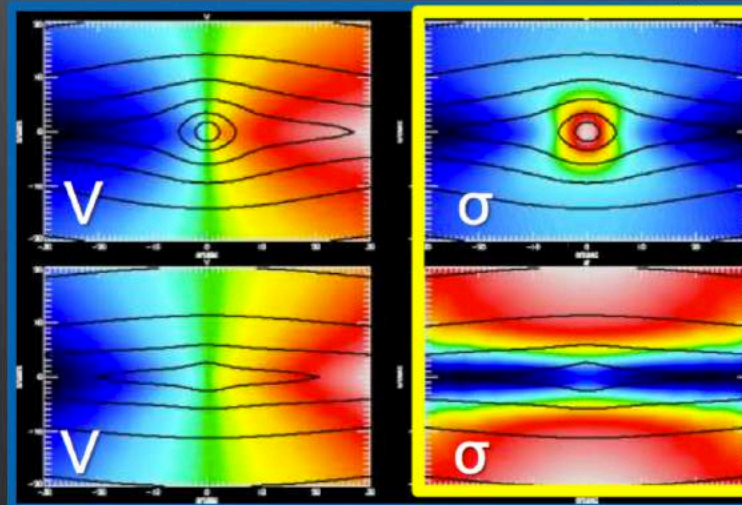
Davies et al. 2001

Why are KDCs special?

- They look cool (great PR)
- They are rare
 - found in early-type galaxies
 - actually, only <11% of early-type galaxies
- Kinematics of majority of galaxies is easy to predict based on their shapes (Cappellari et al. 2013)
- kinematics of KDCs is **not** easy to model



Cappellari 2011, conference talk



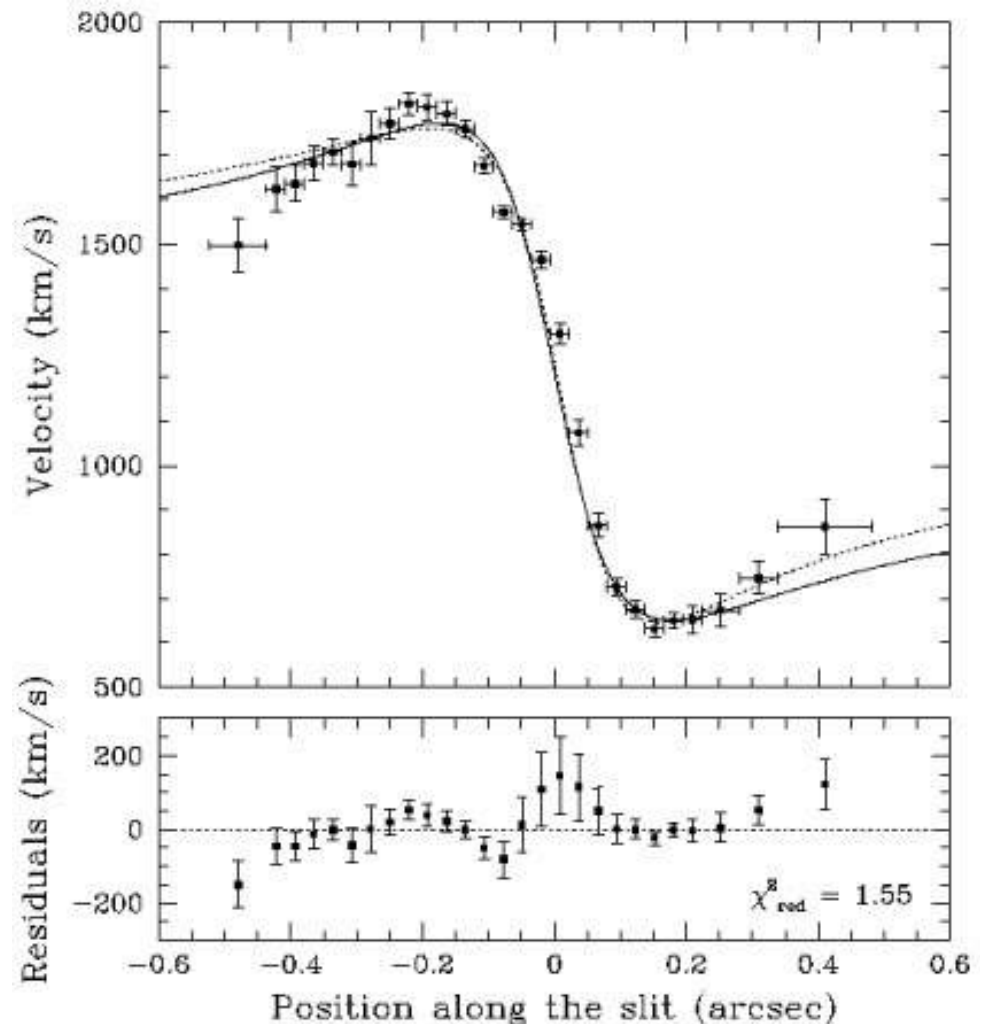
Isotropic model
Bulge mass=10

Isotropic model
Bulge mass=1

ETG: Evidence for central Black Holes

Zooming in further, we can see that the dynamics of the matter near the very center of massive ellipticals shows **evidence of orbiting (super)massive compact objects (SMBHs)**.

Right: Optical emission-line rotation curve for the nuclear disk in M87. The two curves in the upper panel correspond to Keplerian thin disk models, and the bottom panel shows the residuals for one of the models



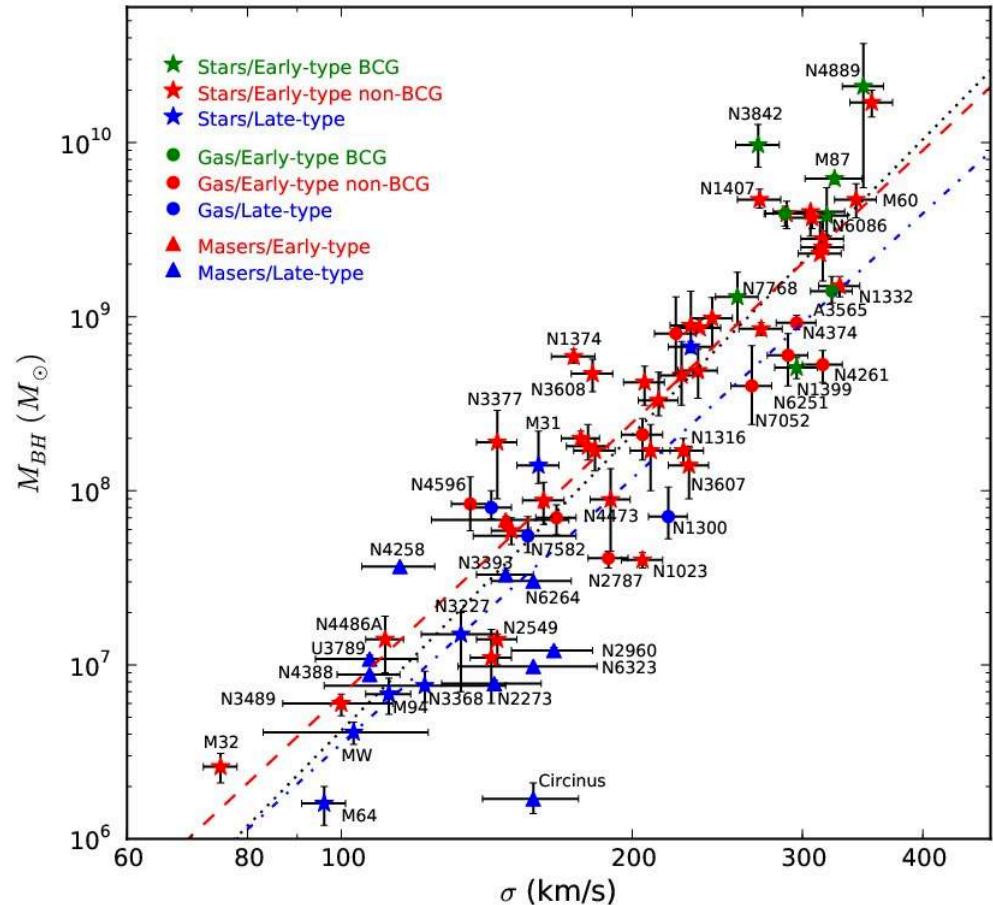
M_{BH}-σ relation

The relation:

$$M_{BH} \propto \sigma^2$$

where M_{BH} is the mass of the central supermassive black hole, σ is the velocity dispersion of the surrounding bulge, and $\gamma = 4$ to 5 (and somewhat dependent on the galaxy type).

Points to a connection between the growth of the SMBH and the surrounding galaxy: SMBH regulates galaxy growth.



Ferrarese, F. and Merritt, D. (2000)

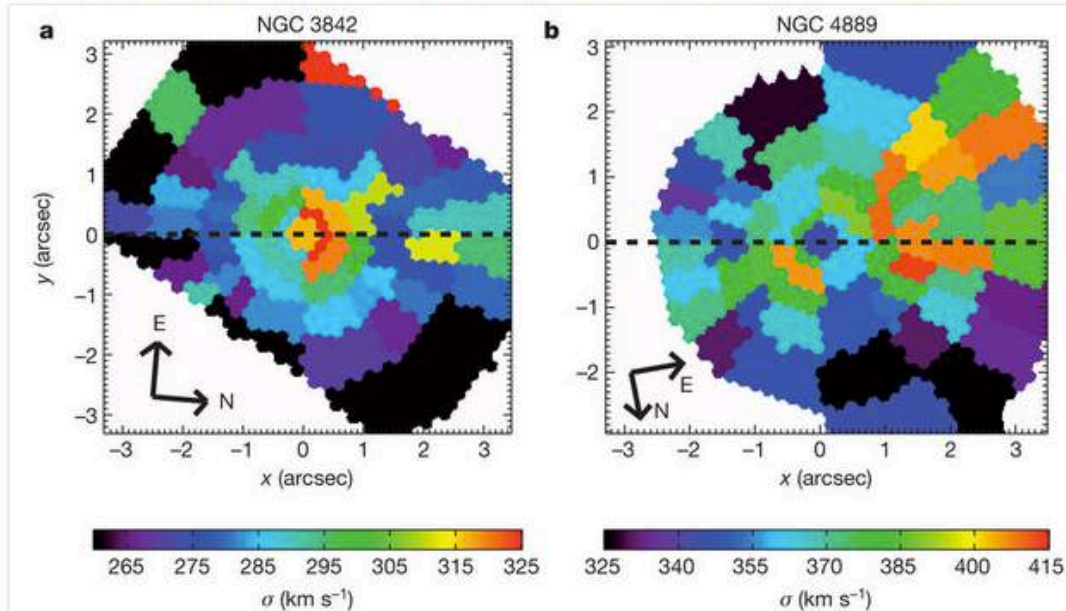
Gebhardt, K. et al. (2000)

<http://adsabs.harvard.edu/abs/2013ApJ...764..184M>

See http://www.astro.wisc.edu/~morsony/150/lectures/lecture16_heinz.pdf for more.

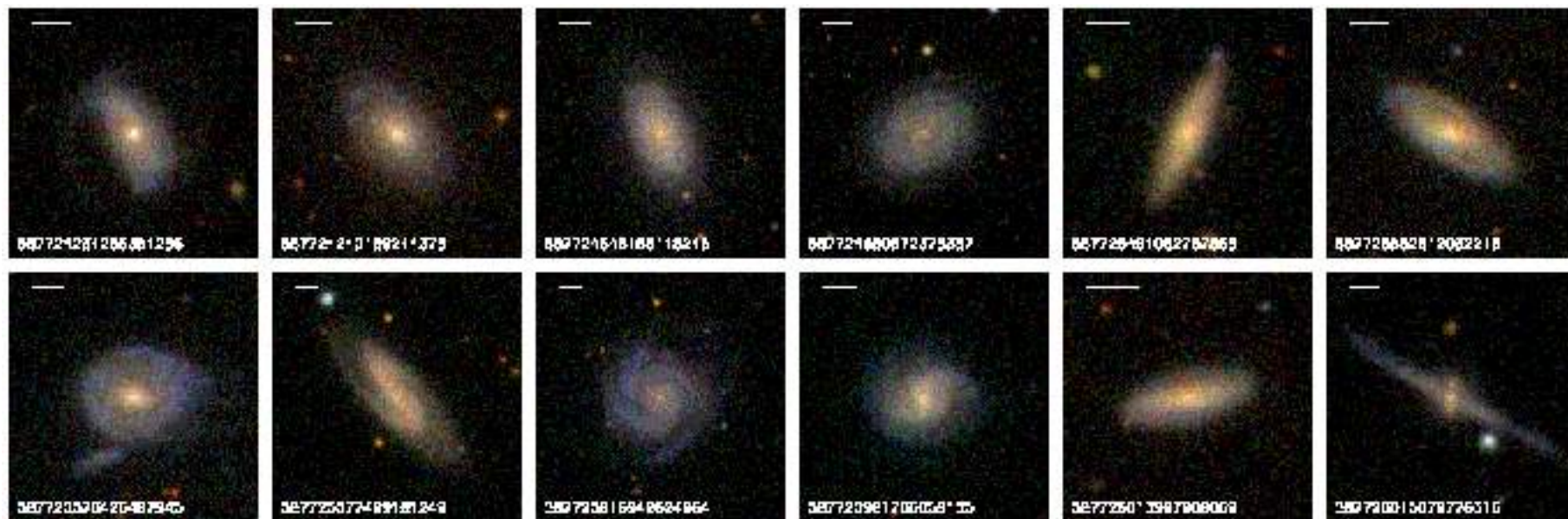
Departures from $M_{\text{BH}}\text{-}\sigma$ relation?

Figure 1: Two-dimensional maps of the line-of-sight stellar velocity dispersions.

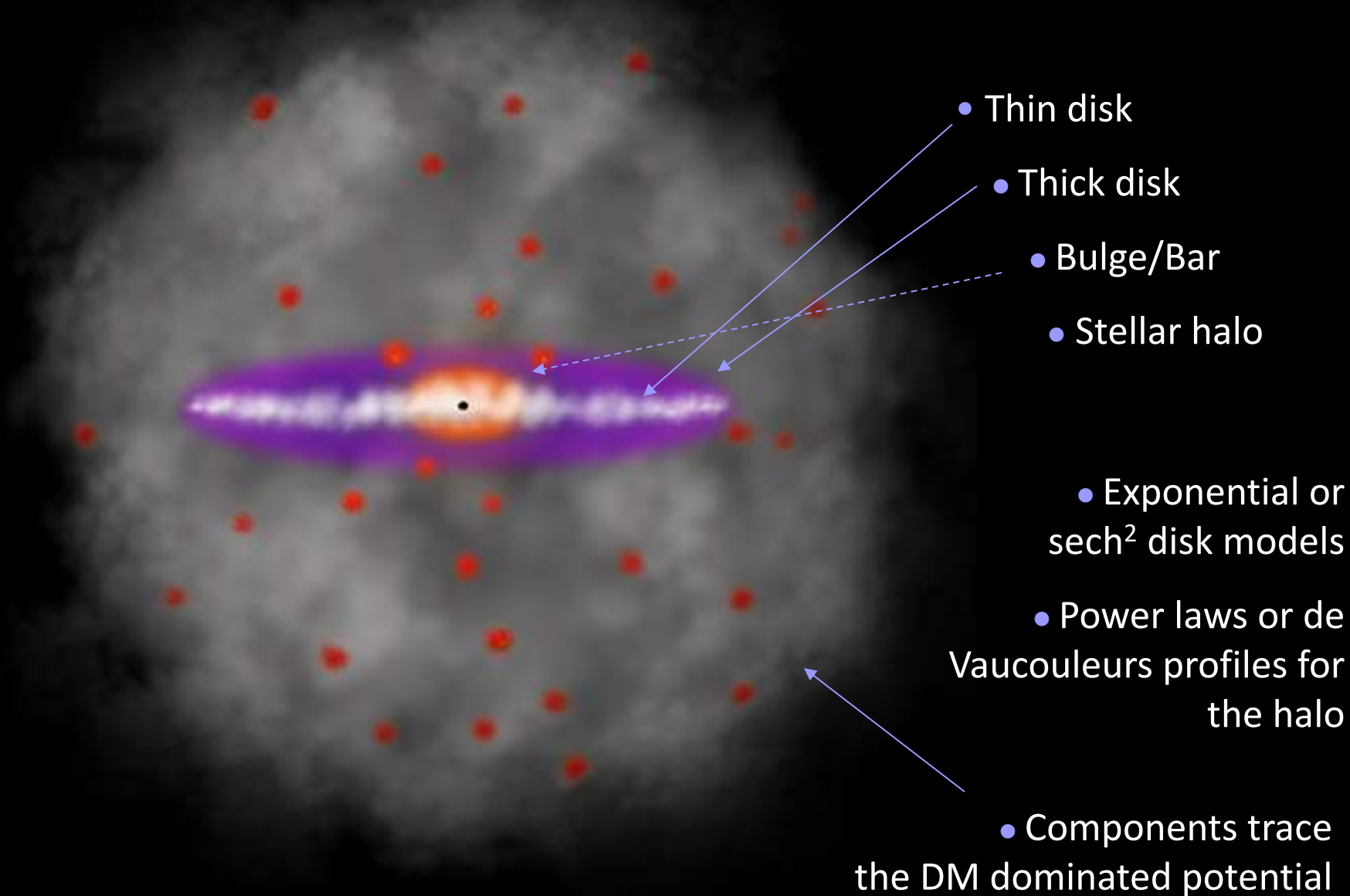


The maps show the central regions of NGC 3842 (a) and NGC 4889 (b) observed using the GMOS spectrograph²³ on the 8-m Gemini North telescope. Additional kinematics at large radii were measured using the VIRUS-P spectrograph²⁴ on the 2.7-m Harlan J. Smith telescope, and additional high-resolution data were acquired with OSIRIS spectrograph²⁵ at the 10-m Keck 2 telescope. GMOS, OSIRIS and VIRUS-P are all integral-field spectrographs, which record spectra at multiple positions in a two-dimensional spatial array. The horizontal dashed line in each panel traces the major axis of the galaxy. The median 1-s.d. errors in velocity dispersion are 12 km s^{-1} and 20 km s^{-1} for NGC 3842 and NGC 4889, respectively. In NGC 4889, the highest velocity dispersions, near 410 km s^{-1} , are located on the east side of the galaxy, at least 1.1 arcsec from the centre.

Late Type Galaxies

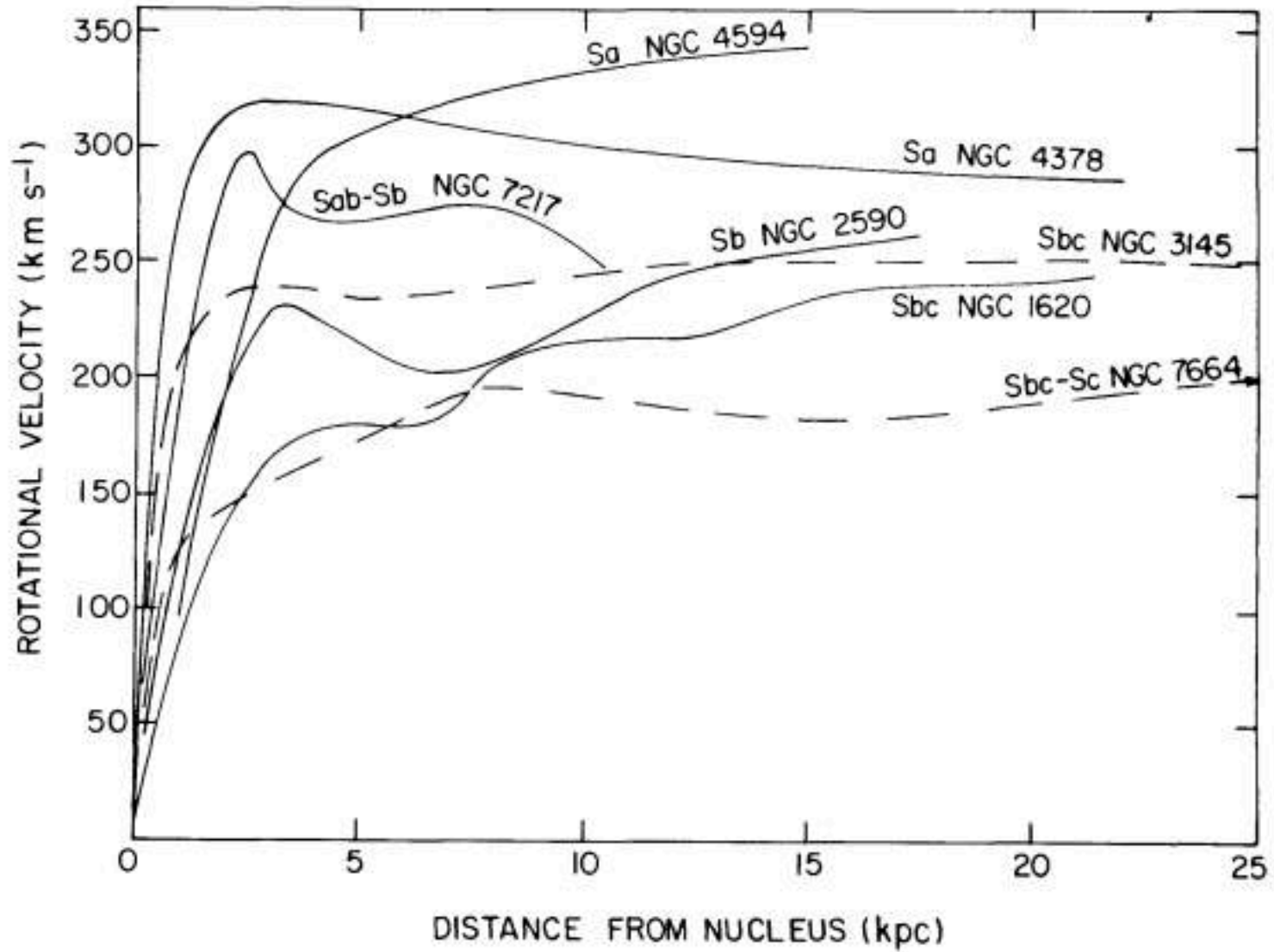


Late Type Galaxies



Kinematics of Disks (Coarse)

- Already discussed in Lecture 3
- Slides 18-26
- Brief recap:
 1. Disks are rotationally supported
 2. Measurements of circular velocity show it remains high even at large radii
 - Points to a need for a dark matter halo
 3. There's an empirical relation of maximum circular velocity and galaxy luminosity: $L \propto v_c^4$



The Tully-Fisher Relation

The (maximum, the flat part value) rotation velocity is related to galaxy's luminosity:

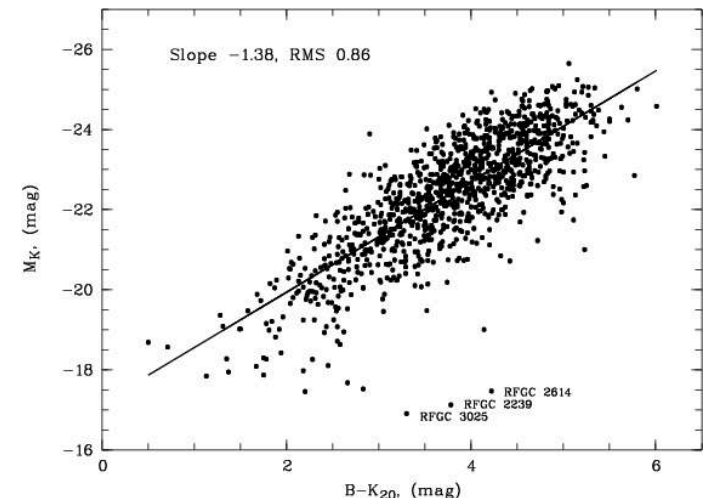
$$M_B = A \log v_c + B \quad (7)$$

where $A \sim -10$ and $B \sim 3$ depend slightly on galaxy's morphological type.

Another way of expressing the same correlation

$$L \propto v_c^{-0.4A} \propto v_c^4 \quad (8)$$

Right: Karachentsev et al. (2002)



The Physics Behind T-F Relation

- Thinking is very similar to that behind the explanation for Faber-Jackson:
 1. Late type galaxies are rotationally supported systems
 2. Their mass-to-light ratios are constant and the same across all late type galaxies
 3. Their surface brightnesses are identical

Kinematics of Disks (Details)

- Kinematics of disks can get incredibly intricate (n.b., partly because we live in one and can observe the action up, close, & personally).
 - Multiple components
 - Moving groups
 - Gradients
 - Changing velocity ellipsoids
 - etc.
- We will return to some of this when we discuss the Milky Way later in the course.

Example: Moving Groups

Example of how proper motions can reveal kinematic structure in the Solar neighborhood (Bond et al. 2009; SDSS data).

The clusters to the left are known as “Eggen’s Moving Groups”; the stars in groups exhibit common proper motions, hypothesized to be the signature of common point of creation (i.e., an open cluster)

These kinds of studies require high astrometric precision, making them difficult to do from the ground (atmospheric seeing).

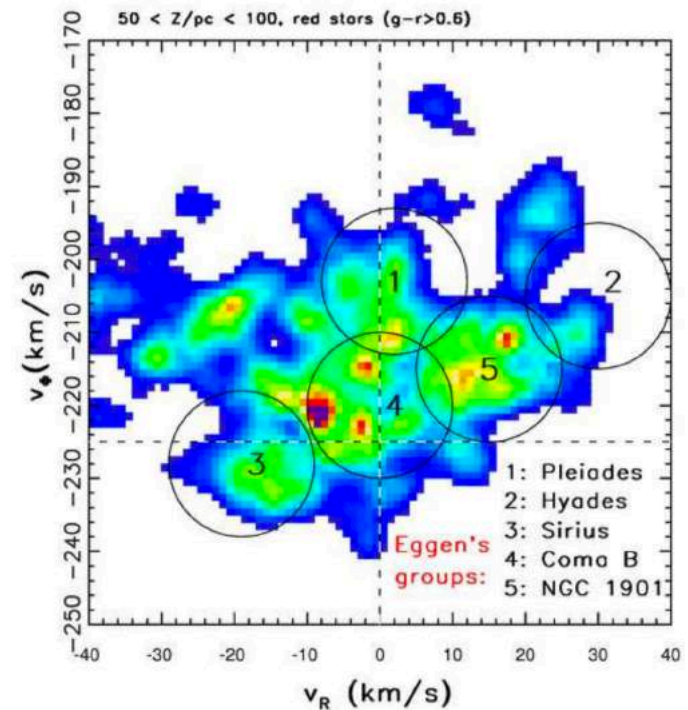
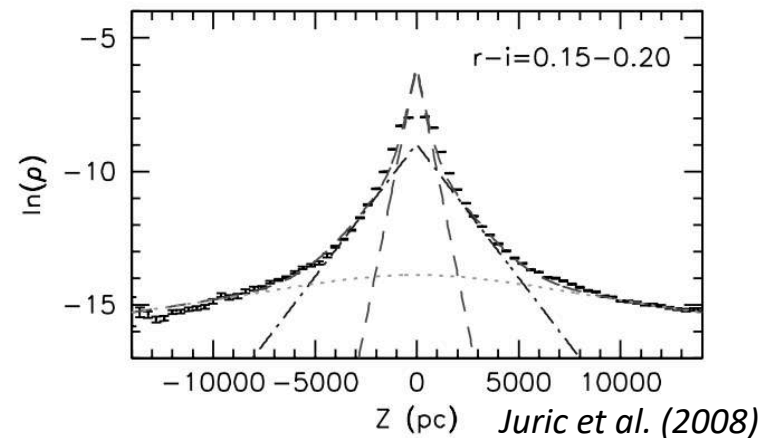
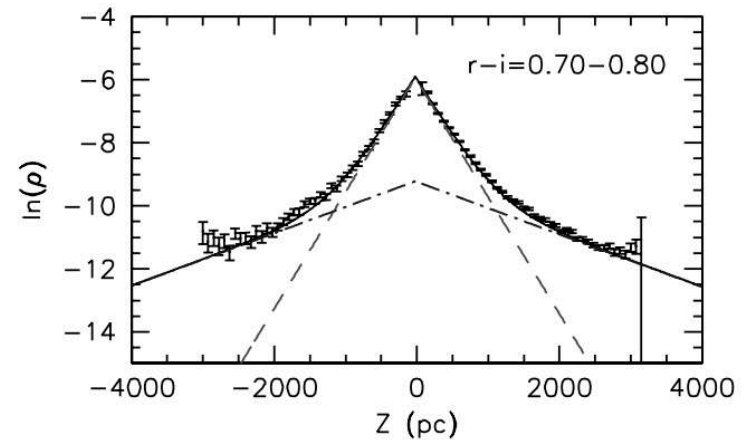
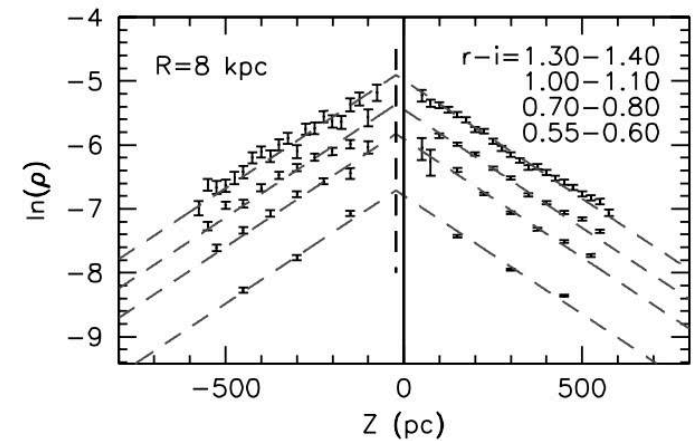


Fig. 4.— Similar to the top left panel in Figure 3, except that stars are selected from a distance bin that corresponds to HIPPARCOS sample ($Z = 50 - 100$ pc). The positions of Eggen’s moving groups (Eggen 1996) are marked by circles, according to the legend in the bottom right corner. The horizontal line at $v_\phi = -225$ km s⁻¹ corresponds to vanishing heliocentric motion in the rotational direction.

The Thick Disk

- Initially discovered through star counts (Bahcall & Soneira 1980)



The Thick Disk

- Initially discovered through star counts (Bahcall & Soneira 1980)
- Kinematics:
 - Higher velocity dispersions (extends higher above the plane)
 - Rotational velocity is lower
 - In the Milky Way, there's no kinematic thin/thick disk dichotomy (e.g. Bond et al. 2009)
- Argues for internal dynamical origin (e.g., via spiral structure driven radial migration – Roskar et al. 2008; Loebman et al. 2008)

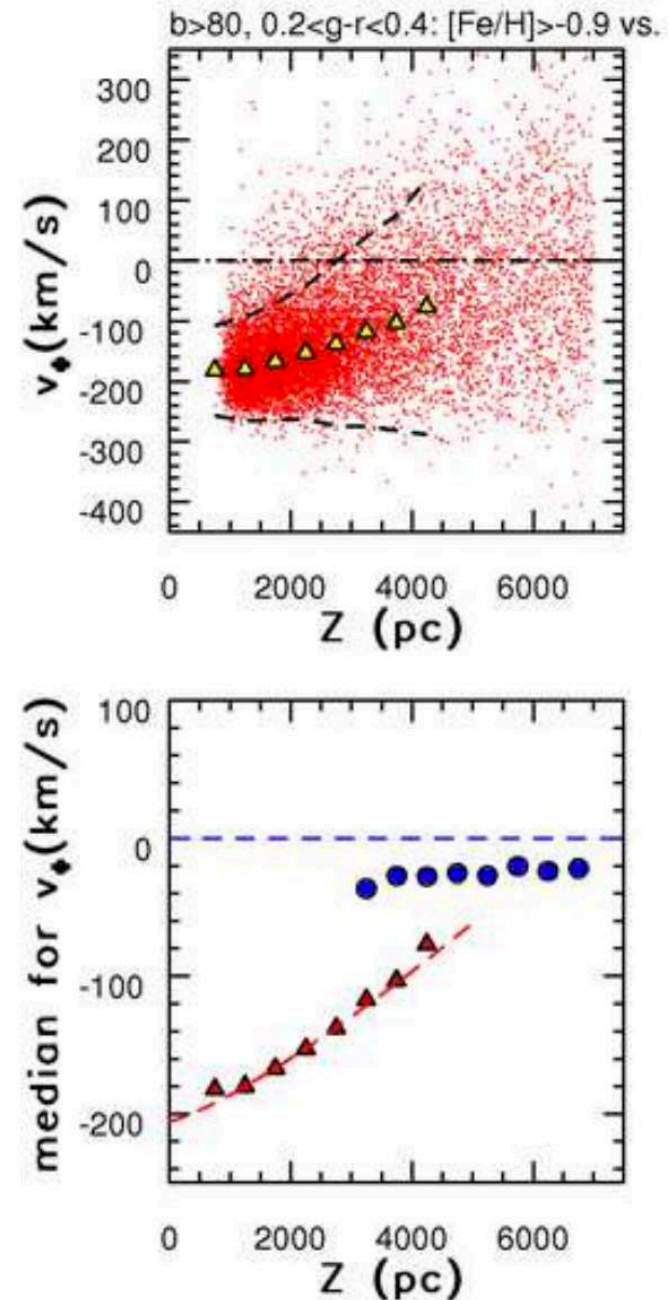


Figure 5, Bond et al. (2009)

Counter-rotating disk components

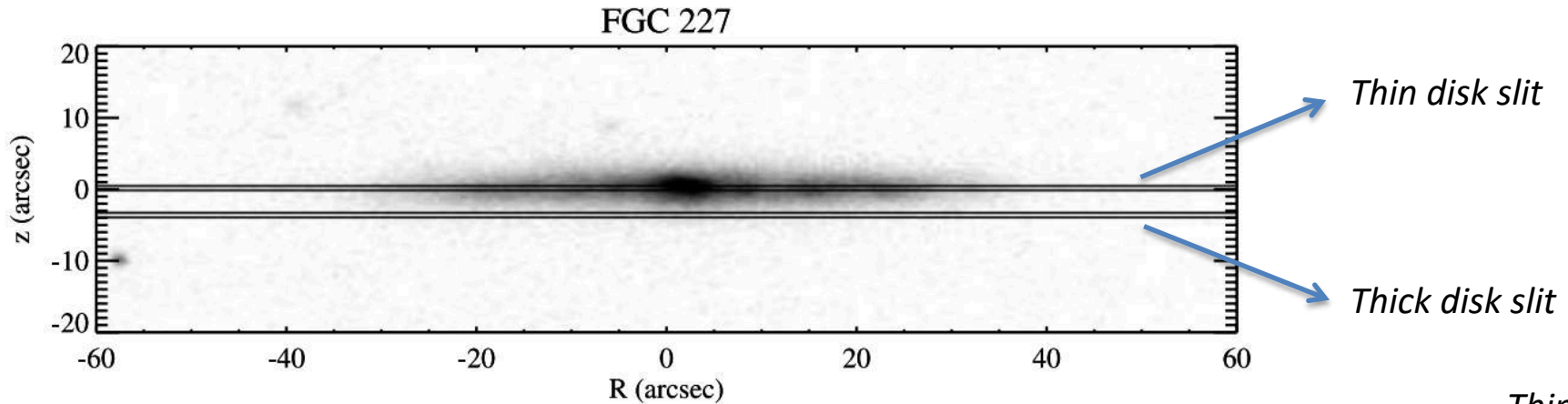


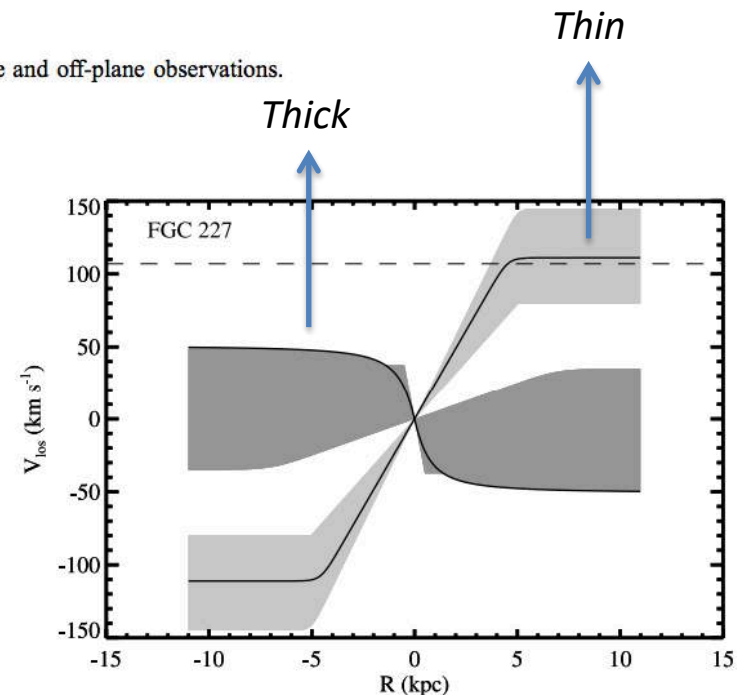
FIG. 2.—*R*-band images of our galaxies, showing the location (*solid lines*) of the slit jaws for our midplane and off-plane observations.

A few spirals appear to show disk components rotating in opposing directions.

These are indicative of external origin of those components (e.g., via galaxy mergers/accretion).

Yoachim & Dalcanton (2005)

<http://iopscience.iop.org/article/10.1086/428922/pdf>



Another Example

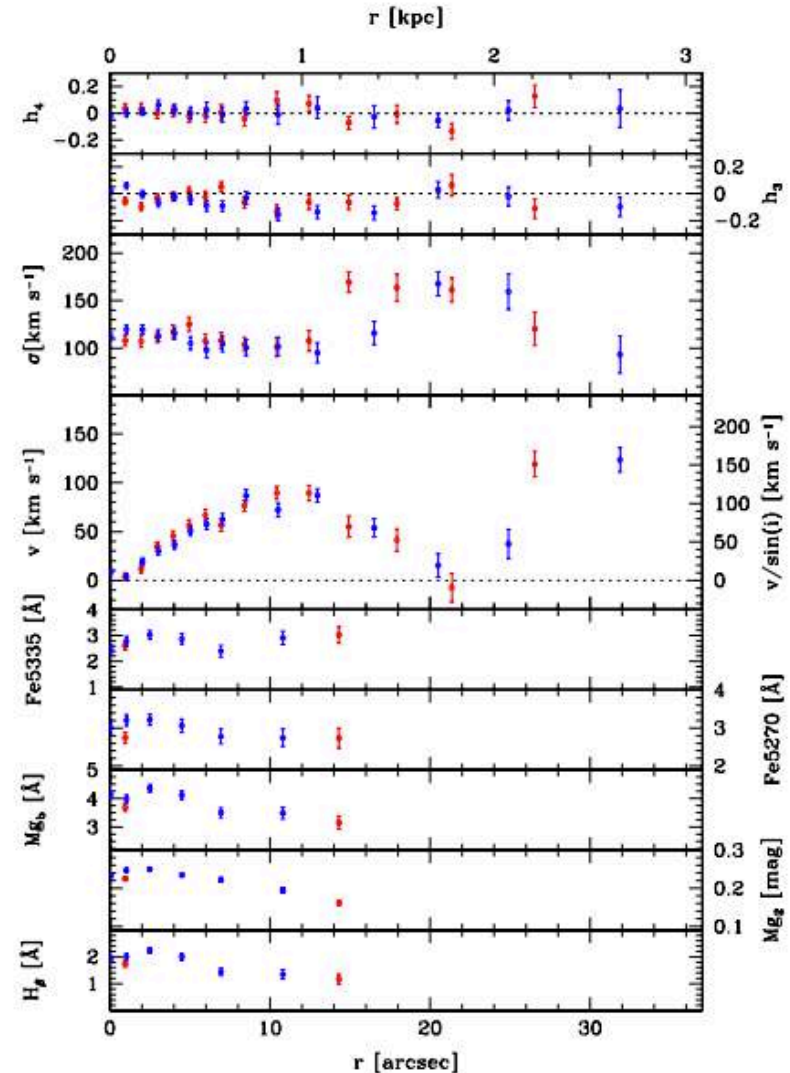
Pizella et al. (2014)

<https://arxiv.org/pdf/1409.3086v2.pdf>

Fig. 1. Stellar kinematics and line-strength indices as measured along the major axis of NGC 4138. The radial profiles of the line-of-sight fourth- and third-order coefficient of the Gauss-Hermite decomposition of the LOSVD (h_4 and h_3); velocity dispersion (σ); velocity (v) after the subtraction of systemic velocity; and the line-strength indices Fe_{5335} , Fe_{5270} , Mgb , Mg_2 , and $\text{H}\beta$ are plotted (from top to bottom). The red and blue dots indicate the receding (NW) and approaching (SE) side of the galaxy, respectively.

Claim counter-rotating components appears marginally younger and associated with star formation -> in situ formation from accreted gas (as opposed to accretion of already formed stars).

Alternative: accretion of gas on filaments (Algorry et al. 2014; Vergani et al. (2007; NGC 5719))



Kinematics of Halo Stars

- Halos make up a small fraction of the total stellar mass ($\sim 1\%$)
- Stars on highly elliptical orbits
- In the Milky Way:
 - Likely (at least) two kinematically distinct components:
 - A smooth component, likely dating back to formation of the milky way
 - A clumpy, accreted, component
 - Details in Ivezić, Beers & Juric (2012)
- n.b.: stellar halo \neq dark matter halo!

Bulges (and Bars)

- Three types of bulges (with different kinematics and formation scenarios)
 - Classical (properties similar to elliptical galaxies)
 - Disky (properties similar to disks)
 - Boxy/Peanut (related to bars)
- See the reviews below for more detail

Internal Kinematics of Galaxies

- Overview ✓
 - Observational methods and constraints ✓
 - Kinematics of Early Type Galaxies ✓
 - Kinematics of Late Type Galaxies ✓
-
- The Milky Way (Lecture 13)
 - Dwarf Spheroidals (Lecture 10)

Next time

- Dynamics!